REPORT DOCUMENTATION PAGE

Form Approved
OMB No. 0704-0188

AD-A252 058

2. REPORT DATE	3. REPORT TYPE AND DATES COVERED
05-15-92	Technical 06-01-91 to 05-31-92

4. TITLE AND SUBTITLE
Adsorption, Diffusion and Epitaxy of Si on Si(100)

5. FUNDING NUMBERS
N00014-81-K-0598

6. AUTHOR(S)
Z. Zhang and H. Metiu

7. PERFORMING ORGANIZATION NAME(S) AND ADDRESS(ES)
University of California
Department of Chemistry
Santa Barbara, CA 93106

8. PERFORMING ORGANIZATION REPORT NUMBER
T11

9. SPONSORING/MONITORING AGENCY NAME(S) AND ADDRESS(ES)
Office of Naval Research
Chemistry Program
800 N. Quincy Street
Alexandria, VA 22217

10. SPONSORING/MONITORING AGENCY REPORT NUMBER

11. SUPPLEMENTARY NOTES
Prepared for Publication in CCAST (World Laboratory) Symposium/Workshop Proceedings, vol. 8

12a. DISTRIBUTION/AVAILABILITY STATEMENT
Approved for public release;
distribution unlimited

12b. DISTRIBUTION CODE

13. ABSTRACT (Maximum 200 words)

We review our recent work on the migration and the self-organization of the Si atoms deposited on a Si(100)-(2X1) surface. The silicon silicon interactions are modelled by the Stillinger-Weber potential, and we use molecular dynamics and Monte Carlo simulations, total energy calculations, as well as phenomenological approaches to study the following topics of current interest: the effects of surface reconstruction-unreconstruction on the adsorption dynamics; the spatial distribution of the adsorbate in the early stages of deposition; the migration of an adatom on a terrace or across a step; the role of adatom-adatom interactions in the formation of anisotropic islands; the transformation of a surface with single layer steps to one with double layer steps; the effects of kink-kink interaction in step roughening, etc. Wherever possible, the results obtained are compared with findings of recent experiments; we find that our qualitative conclusions are in agreement with the STM observations.

14. SUBJECT TERMS	15. NUMBER OF PAGES
	60
	16. PRICE CODE

17. SECURITY CLASSIFICATION OF REPORT	18. SECURITY CLASSIFICATION OF THIS PAGE	19. SECURITY CLASSIFICATION OF ABSTRACT	20. LIMITATION OF ABSTRACT
Unclassified	Unclassified	Unclassified	UL

OFFICE OF NAVAL RESEARCH

Contract N00014-81-K-0598

R&T Code N47092

Technical Report No. 11

Adsorption, Diffusion and Epitaxy of Si on Si(100)

by

Z. Zhang and H. Metiu

Prepared for Publication in

CCAST (World Laboratory) Symposium/Workshop Proceedings, Vol. 8

May 15, 1992

ADSORPTION, DIFFUSION, AND EPITAXY OF SI ON SI(100)*

ZHENYU ZHANG and HORIA METIU

Department of Chemistry and Physics
University of California
Santa Barbara, CA 93106, U.S.A.

ABSTRACT: We review our recent work on the migration and the self-organization of the Si atoms deposited on a Si(100)-(2X1) surface. The silicon silicon interactions are modelled by the Stillinger-Weber potential, and we use molecular dynamics and Monte Carlo simulations, total energy calculations, as well as phenomenological approaches to study the following topics of current interest: the effects of surface reconstruction-unreconstruction on the adsorption dynamics; the spatial distribution of the adsorbate in the early stages of deposition; the migration of an adatom on a terrace or across a step; the role of adatom-adatom interactions in the formation of anisotropic islands; the transformation of a surface with single layer steps to one with double layer steps; the effects of kink-kink interaction in step roughening, etc. Wherever possible, the results obtained are compared with the findings of recent experiments; we find that our qualitative conclusions are in agreements with the STM observations.

* To appear in CCAST (World Laboratory) Symposium/Workshop Proceedings, Vol. 8, *Surface Physics* (Gordon and Breach, London, 1991).

1. INTRODUCTION

For technological and scientific reasons one would like to have a better understanding of the kinetic processes taking place during epitaxial deposition on semiconductor surfaces. The bulk of our information comes from electron scattering measurements[1,2] performed *in situ* during growth. If the deposition is made on a flat surface the main issue is whether the growth is two or three dimensional. Two dimensional growth means that the crystal is grown layer by layer. During the deposition *one-atom-high* islands grow and join each other to form a surface layer, before a significant number of atoms will be trapped on top of them. Three dimensional growth is opposite. New one-atom-high islands grow on older one-atom-high islands, which have grown on older islands, etc. Four to five layers are simultaneously being completed. Electron scattering can distinguish between these two growth regimes because they lead to a different evolution of surface roughness. During three dimensional growth the surface is *always* rough; during two-dimensional growth the roughness of the surface oscillates: it is highest when a half layer is deposited and lowest whenever a new layer is completed. Since rough surfaces diminish specular (or diffractive) scattering (electron[1,2] or helium[1]), the specular (or any diffracted) beam intensity oscillates if the growth is two dimensional.

The substrate surface is not always flat. Often the presence of steps is unavoidable, and recently vicinally cut substrates have been deliberately used for the growth of new structures. The growth on such stepped surfaces has new features. If the atoms falling on the terrace have high mobility they reach a nearby step before they have a chance to meet each other on the terrace. If they stick to the step, the deposition causes step propagation.[3,4] In the opposite limit the atoms form islands on the terraces.[4,5] Step propagation causes no change in surface smoothness or in the periodicity of the steps. Therefore, the diffraction spots due to terrace periodicity persist throughout the deposition and the intensity of the specularly scattered beam is unaffected. Two dimensional island growth on terraces causes atomic level roughness on the terrace until the deposition of a

monolayer is completed. The diffraction spots characteristic of step periodicity, and the high intensity in the scattered beam (characteristic of surface flatness), deteriorate as the coverage is increased and recovers when one layer is completed.[6,7]

In the case of multicomponent systems (e.g. Ga and Al deposition on stepped GaAs surfaces) the step can induce chemical segregation (e.g. Al segregates near the step and Ga on the remainder of the terrace).[8] One would like to know when and how such segregation takes place, and how smooth is the border between the phases.[9]

From the point of view of the atomic theory the information provided by these experiments is rather crude. Therefore, it is perhaps most reasonable to try to understand them by using kinetic simulations in which the adsorbed atoms undergo jumps on a square lattice and interact with each other by simple rules.[9-14] The influence of the finer details, such as the reconstruction of the surface, the presence of multiple adsorption sites, and the complicated nature of the interatomic potentials, are left out of the investigation. While important, such simulations are not reviewed here.[15]

The development of the scanning tunneling microscope (STM) made it possible to investigate surface growth at an atomic level. STM is not yet an universal tool: no measurements have been as yet performed under the high temperature conditions used in epitaxy and the pictures taken on some of the practically interesting materials do not show much detail. There is reason to believe that these shortcomings are temporary. On the other hand, for the surfaces and the conditions for which STM works well the quality of the information is astonishing.

An example of what is possible is provided by the recent STM studies[3-5,13,16-22] of the Si(100) surface covered with adsorbed Si atoms. These measurements have determined the adsorption sites on the surface; studied the shape of the islands formed by a small number of atoms; investigated how the shape of the steps changes under the influence of heating or atom deposition; determined the configuration of the three dimensional islands; and provided complete statistical information on step roughness.

Theory can explain these observations only by using models which incorporate the atomic details: surface reconstruction, the location of the adsorption sites, the barriers between them, realistic adsorbate - adsorbate interactions, etc.

In this article we review our group's efforts[23-28] to provide a qualitative (or semi-quantitative) understanding of the results obtained by STM measurements on the Si(100) surface. For the sake of simplicity we deal with processes that either involve isolated adatoms, or low coverage. This is a first step towards a comprehensive study of growth kinetics.

Because of the length of the article it is useful to summarize our main findings and explain how the material is organized. All the results presented here are obtained by using molecular dynamics, Monte Carlo simulations or total energy calculations with the silicon-silicon interaction proposed by Stillinger and Weber (SW).[29] As will be discussed in more details, there are many other empirical potentials available for Si, and density functional and tight binding calculations are also becoming practical. Unfortunately, there is no proof that any of them describes all silicon properties adequately. A specific version obtained by fitting a specific set of data turns out to be particularly good at describing several properties of the system, but fail with others. We use the SW potential because it is qualitatively reasonable: it reproduces well most of the bulk properties of solid and liquid Si, and many of the properties of the Si(100) surface. Our qualitative conclusions that can be tested experimentally are in agreement with the observations. Additional information on the potentials is given in Section 2.

In Section 3 we study the dynamics of single atom adsorption and determine the absorption sites.[23,24] We were surprised to find that there are all together thirteen possible absorption sites, within the (1X2) unit cell of the reconstructed Si(100) surface shown in Fig. 1. Similar calculations based on the density functional method[30,31] or the Tersoff potential[32,33] also suggest a large number of adsorption sites, but they differ in the precise location and binding energy. At the present time it is not possible to conclusively decide which gives a better description of the real system.

One might naively think that the incoming atoms prefer to bind

to the site with the highest binding energy, which is favored by thermodynamics. This is not the case. In our simulations we observe a highly inverted population: the site with the highest binding energy is not reached by direct absorption and one of the thermally metastable sites (with low binding energy) has the highest occupation. While interesting, this phenomenon does not affect growth kinetics since site to site hopping restores the thermal population within microseconds.

In Section 4 we estimate the site to site hopping rates and discuss the nature of single atom migration on a lattice with multiple sites in the unit cell.[24,25] We find that the migration of an atom on the Si(100)-2X1 surface is *highly anisotropic*. Qualitatively it can be described as an one-dimensional random walk on top of a substrate's dimer row (See. Fig. 1), with brief side trips to a site located at the flank of the row.

After hundreds of thousands of such random jumps the atom can get trapped at a site with high binding energy, located between the rows. This migration can be described by a diffusion equation only on a time scale shorter than the time in which the atom is trapped. The diffusion coefficient is a complicated function of the jumping rates between the many sites involved. Since each rate constant satisfies an Arrhenius formula with a different barrier and pre-exponential, the temperature dependence of the diffusion coefficient does not have an Arrhenius form. However, it turns out that within the narrow temperature range employed in crystal growth, the temperature dependence of the diffusion coefficient is well fitted by an Arrhenius formula. But, except for special cases, the activation energy and the pre-exponential differ from those of the site to site jumping rates.

The anisotropy of migration predicted by our calculations is consistent with Lagally's data.[5,13] Lu and Metiu[13(b)] presented simple chemical arguments that suggested that such anisotropy exists on the (100) faces of all materials with diamond or zincblende structure.

In most surface science systems the adsorbed atoms interact more strongly with the substrate than with each other. Because of this the hopping rates are not radically altered by coverage. This is

not the case for silicon. The studies presented in Section 5 show that the rate of jumping from one site to another is very strongly affected by the occupation of the neighboring sites.[26] This dependence is not simple. For example, it is not a function only of the number of atoms surrounding a given site but it strongly depends on the precise position of the occupants.

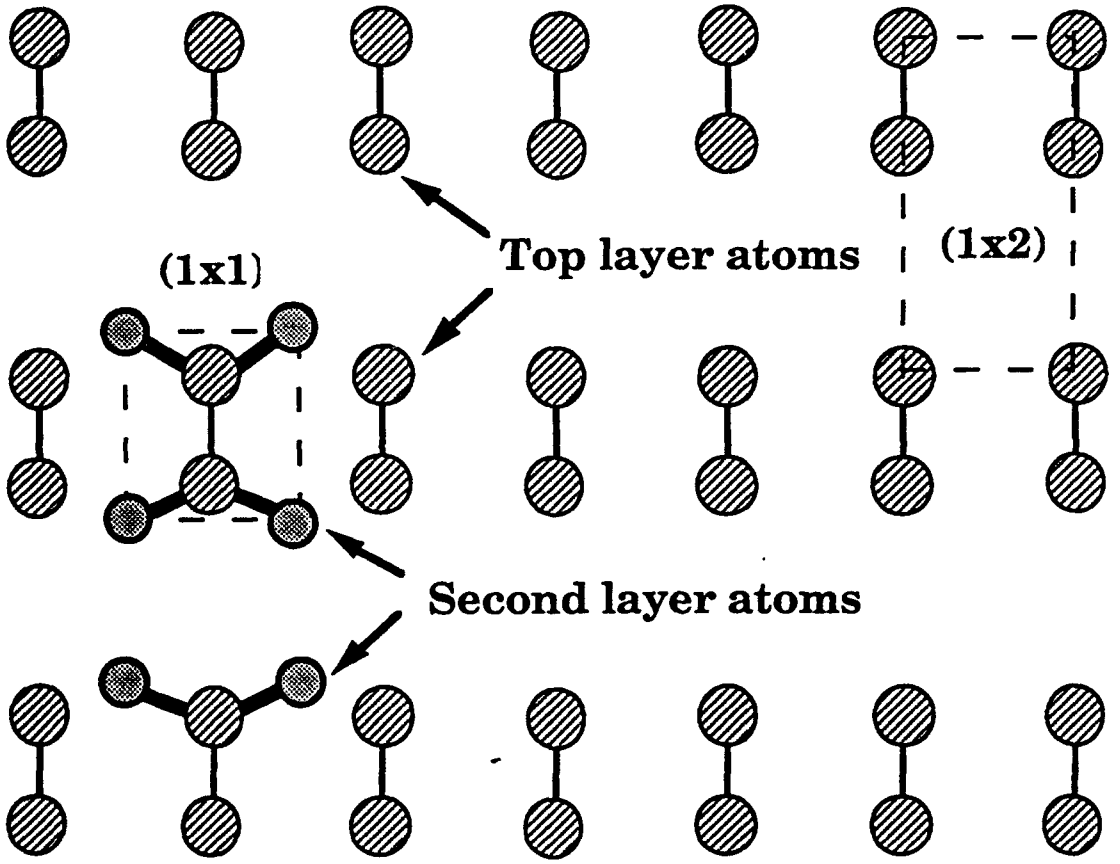

Fig. 1.

The STM pictures show that a small number of atoms deposited on the surface aggregate into thin long islands perpendicular to the substrate's dimer rows.[16,17] The borders of these islands are unusually smooth. Moreover, it is extremely puzzling to see that the

long coast of the island is *perpendicular* to the direction of rapid migration. This means that even though the single atoms on the surface are most likely to make contact with the long coast of an island, there is a mechanism that transports them on the short shore where they stick and increase the island's length. The calculations reported in Section 5 find that an atom arriving at the long coast is likely to climb up on the island and travel along the shore towards the island's end. In this trip the atom can either fill the vacancies along the border, making it smooth, or reach the end, descend onto the substrate and stick to the end of the island making it longer.

The motion of adsorbed atoms on stepped surfaces are of great interest because they are often used as a substrate in epitaxy (e.g. to grow tilted superlattices[8]). Often steps are present on a surface even when they are unwanted; it seems that it may be impossible to cut a Si(100) surface without steps. Finally, even if the substrate surface is step free, subsequent deposition creates islands and the borders of these islands are steps. For these reasons we have studied in some detail in Section 6 the motion of the Si atoms along and across steps.[27]

Our main purpose is to understand a striking experiment performed by Hoeven *et al.*[3] They deposit half a monolayer of silicon on a Si(100) surface which has single-atom-high steps. The absorbed atoms migrate to form a surface having exclusively double-atom-high steps. To do this, the atoms must leave every other terrace and congregate on the terraces in between. Our calculations suggest a kinetic mechanism for this process. On a surface with steps having a single atom height the terraces are not equivalent:[34] the dimer rows on one type of terrace are perpendicular to the step; on the other they are parallel to it. These terraces alternate: a terrace of a given type is always sandwiched between two terraces of the other type. The atoms landing on a terrace can rapidly reach the border if the dimer rows on the terrace are perpendicular to the steps. This happens because the mobility of the adsorbed atoms is highly anisotropic and takes place along the dimer rows.[5,13,24-26,30-32] Our calculations[27] show that when such atoms reach the border there is a significant probability that they will cross it and move on the neighboring terrace. The atoms on terraces having dimer rows parallel to the steps bordering them tend to move parallel to the steps

and have a low probability of reaching the border. Therefore they tend to remain on the terrace on which they landed. As we show in Section 6 these two observations explain why the deposition of half a monolayer of silicon on the stepped surface turns all the single atom high steps into double atom high ones.

The last Section is concerned with the observation that the single-atom-high steps that are perpendicular to the dimer rows on the terrace above them are very rough and have a large number of irregular kinks.[28] Lagally's group[22] has used the STM pictures of these steps to determine the probability of finding kinks of a given height and a given distance between the neighboring kinks. They have also shown that the observed distribution can be fitted reasonably well by a model which assumes that the energy to create a kink is proportional to the kink length and is independent of the nature of the neighboring kinks. Here we show that the agreement with the data is improved when we take into account phenomenologically the kink - kink interactions.[28] Moreover, at a more microscopic level we find that when the dimer row on a terrace are perpendicular to the step below, the step growth is rather peculiar. To a first approximation each dimer row grows independently. This lack of correlation between the row growth leads to step roughness.[27]

2. MODEL POTENTIAL AND METHODOLOGY

Throughout this paper we use the potential proposed by Stillinger and Weber (SW).[29] This has a pairwise part whose main function is to describe the energy needed to stretch a bond, and a three body interaction whose role is to keep the bonds at the correct angle. Furthermore, each Si atom has a propensity to form tetrahedral bonds. Calculations based on this potential reproduce well the properties of the bulk liquid or solid silicon[29] and give reasonable results[35,36] for the structure of the (100)-2X1 surface. It fails however to give the reconstruction of the (111) surface[36,37] and has a mixed success[37] in reproducing the structure and the energy

of small clusters given by *ab initio* calculations.[38] Several modifications have been made to improve the success of the potential for specific applications,[39-41] but here we use the original potential. Some authors believe that the SW potential tends to fail when dealing with over or under coordinated atoms,[37] but that it is adequate for "qualitative" studies of the properties of the (100) surface.

There are many other methods for calculating the interatomic forces. A large variety of functional forms were proposed by Keating,[42(a)] Pearson *et al.*,[42(b)] Takai *et. al.*,[42(c)] Tersoff,[43] Biswas and Hamann,[44] Dodson,[45] Brenner and Garrison,[46] Chelikowski *et. al.*,[47] Khor and Das Sarma,[48] and Bolding and Anderson.[37] To these we add electronic structure methods[49] (which are often of uncertain accuracy) including those used simultaneously with the molecular dynamics calculations, such as the imbedded atom,[50] the Car-Parinello[51] and tight binding [52] methods.

Very few calculations of the quantities of interest here have been performed with other methods. The binding energies for a single adsorbed Si atom and the energy barriers between the adsorption sites have been calculated with the density functional method[30,31] and a modified Tersoff potential.[33(b)] Their results are in qualitative agreement with those found here but the magnitudes of the barriers between sites and the precise position of the binding sites differ. At this time there is no reason for preferring one method over the others.

The existing experiments cannot be used as a decisive test of the quality of a given potential, since there are as yet no "zero coverage" measurements that would allow determination of the energy barriers with a high degree of confidence. The efforts to infer a diffusion constant out of high coverage measurements use rather sophisticated modeling whose validity is uncertain. Moreover, the migration at higher coverages is rather complicated and it may have little connection to the mobility of isolated atoms.

The main purpose of the calculations presented here is to suggest a kinetic mechanism through which the growth patterns observed on the Si(100) surface are generated, rather than to evaluate precisely the binding energies of all the adsorption sites and the

magnitude of the barriers between them. In such a pursuit it is often sufficient to find out which jumps are the most frequent, without having to know the precise numerical values of the jumping rates. The fact that our calculations lead to growth patterns that are very similar to those observed experimentally is pleasing; while this might indicate that the SW potential is chemically reasonable, it does not imply that it is accurate. Further testing of the suggestions made here by detailed STM measurements is highly desirable.

An extremely important practical feature of molecular dynamics and Monte Carlo calculations is the need to make an enormous number of evaluations of the potential energy. Even though we have optimized these calculations and the SW potential is relatively simple, we are frequently straining the available computer power. A potential in which increased accuracy is obtained at the expense of the evaluation time, is not a practical option.

3. ADSORPTION

A study of Si adsorption on Si(100)-2X1 surface should answer several questions: (1) What are the binding sites for a newly adsorbed atom? (2) Does the adsorption of a single atom change the structure of the surface layer? (3) How are the incident and the binding energy of the incoming atom dissipated when sticking takes place? (4) Are there any low coverage collective effects?

In many cases, the deposition of an atom on a reconstructed surface will induce interesting displacements in the surface layer. As more and more atoms are deposited, the surface layer becomes a sub-surface layer. At some point during deposition the former surface atoms must unreconstruct and take the bulk equilibrium positions.

This transition can take place in two different ways. If may be a phase transition in which a large number of newly deposited atoms are needed to induce the collective rearrangement of a large group of surface atoms. The alternative is that the unreconstruction of the surface is a local effect determined mainly by the interaction between the newly arrived atom and the nearby surface atoms. In this case

the unreconstruction takes place on a first come first served basis, and should be observable in the early stages of the deposition studied here.

3.1. Single Atom Adsorption Dynamics

In studying the adsorption dynamics we model the surface by a cluster of 99 atoms, distributed in five layers.[23] When molecular dynamics calculations are performed 14 atoms are propagated by solving Newton's equations, and 29 obey a Langevin equation using the correct potentials, a local memory-less friction and a Gaussian random force related to the friction through the customary fluctuation-dissipation theorem. The rest of the atoms in the cluster are held fixed and provide a template for the atoms that are moving.

Prior to the deposition of a new atom, the substrate atoms that will be allowed to move during the MD simulation are relaxed to their equilibrium positions by using the Metropolis Monte Carlo procedure.[55] The relaxation is carried out at the temperature of 500 K, which is close to 570 K, the temperature at which good quality epitaxial growth has been observed.[1]

We choose the center of a surface dimer to be the origin of the xy-plane. The plane of the centers of the outermost atoms before surface reconstruction defines z=0. The incident Si atom starts at a position (0, 0, z) well above the surface, where the interaction energy between the incident atom A and the surface is practically zero. The initial velocity of A is perpendicular to the surface and its magnitude is sampled from a Maxwell - Boltzmann distribution at a specified temperature. For each trajectory, the active substrate atoms start from a spatial configuration produced by Monte Carlo sampling, with velocities sampled from a Maxwell - Boltzmann distribution.

We denote by T1 and T2 in Figs. 2(a) and 2(c) the sites occupied by the atoms of a newly deposited, defect free surface layer. Our calculations show that an incident atom aimed at the site T1 breaks the dimer bond, inserts itself into the dimer and gets trapped there. In the final configuration which we call a trimer (see Fig. 2(e)), the

two atoms formerly engaged in the dimer move to their equilibrium bulk positions, with the adatom residing at the apex.

This direct insertion dimer opening mechanism takes place frequently, and is insensitive to the simulation parameters used. We have independently varied the temperature of the incident atom and the surface temperature from 0 to 500 K, and the impact parameter was sampled to cover uniformly the square $|x|, |y| < 0.77$ Å (Fig. 2(a)). In all cases at least 50% of the trajectories form a trimer by direct insertion into the dimer. The direct insertion mechanism for adsorption and dimer opening was also observed recently by Srivastava and Garrison using the Tersoff potential,[32] while in earlier simulations its importance has not been emphasized.[56,57]

The Stillinger - Weber potential gives a dimer bond strength of nearly 2 eV. This bond is broken simultaneously with the formation of two new bonds between the incident atom and the atoms that used to form the dimer. Thus, the insertion of the incident atom is exothermic.

Initially most of the energy released by the formation of new bonds is localized on the trimer as vibrational energy, and it is transferred to the lattice on a time scale longer than a picosecond. After insertion, the incident atom oscillates, mostly in the direction perpendicular to the surface; the surface atoms initially bound in the dimer oscillate, after the trimer formation, mostly parallel to the surface.

An incident atom that does not break the dimer bond is most likely to end at an F^0 site (see Fig. 3(a)). It can get there in two ways. The incident atom knocks off one surface atom from a dimer and places it at the site F^0, as shown in Fig. 3(a); the incident atoms pairs up with the surface atom left behind (see Fig. 3(a)) to reform the dimer. Or, the incoming atom is deflected by the dimer and settles at the F^0 site. The atom at the site F^0 is 0.5 Å *below* the surface layer, and is unable to open the neighboring dimers to form a trimer. Instead, the two neighboring dimers are slightly pushed away from their 2X1-(100) equilibrium positions.

The incident atoms aimed at the site T2 (Fig. 2(c)) have a

tendency to stick at the site F^* (see Fig. 3(b)). An atom in that position is unable to break the bonds of the neighboring dimers and induce the unreconstruction shown in Fig. 2(d). It only manages to pull the neighboring dimers closer to the F* site by a distance of about 0.4 Å. F^* differs from F^0 only through its z-coordinate; z_{F^*}= 1.0 Å and the F* site is, unlike F^0, above the surface but below the apex of a trimer.

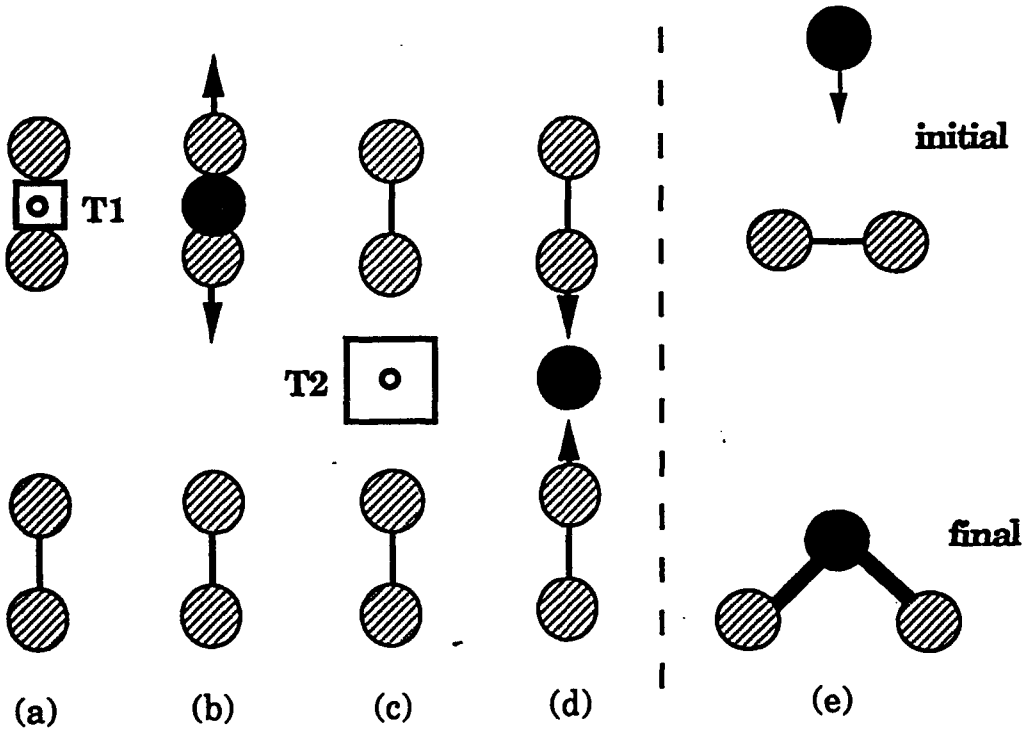

Fig. 2. T1 and T2 indicate the location of the deposited atoms after the deposition of a monolayer. (b) and (d) show possible surface atom displacements caused by the adsorption. Only (b) takes place during the formation of the trimer shown in (e). The solid circles represent adatoms; the stripped are the substrate's surface atoms.

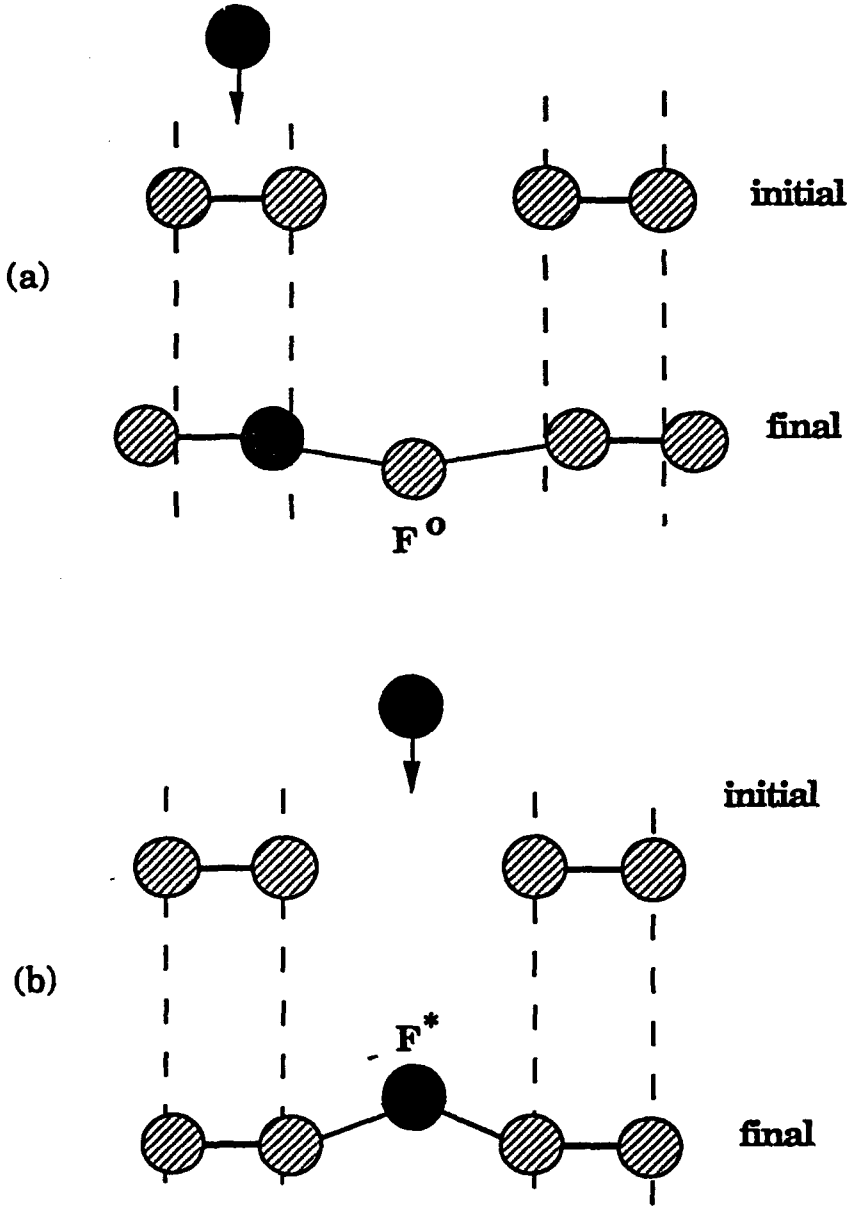

Fig. 3. Adsorption processes leading to the occupation of the bridge sites between two dimer rows. F^0 in (a) is below the surface layer; F^* in (b) is above the surface layer.

3.2. Collective Effects

As noted above, an atom adsorbed half way between two dimers is either below the surface (if adsorbed at F^0) or above the surface (at F^*) but below the new layer. In addition, such an adatom is unable to pull the nearby surface atoms out of position and form a trimer with them. Since trimerization must take place by the time the deposition of a monolayer is completed, we infer that the atoms that happen to stick to the F^* or the F^0 positions can only induce trimerization if assisted by atoms deposited subsequently.

In searching for such a collective effect, we have placed an atom A1 at F^0 and performed a large number of MC moves to make sure that all surface atoms were in positions compatible with thermal equilibrium. This means that they were located at positions generated by importance sampling, not at the mean equilibrium positions.

After the equilibration is completed we aim an atom A2 at T1 with a thermal velocity perpendicular to the surface, as shown in Fig. 4(a). Many of these trajectories lead to the trapping of A2 at the center of the dimer, labeled as the B site. This breaks the dimer bond S3 - S4, and the trimers S2- A1 - S3 and S3 - A2 - S4 (see Fig. 4(b)) are formed. The atoms in these trimers relax to their bulk-like positions; compared to the initial configuration, the distance S3 - S4 is longer, S2 - S3 is shorter, and A1 is lifted up. Notice that the dimer S1 - S2 is unaffected: S1 follows S2 and maintains its dimer bond with it.

Similar collective effects are observed if we initially place an atom in equilibrium at F^* and send a second atom at B.

These collective effects resemble those observed by Srivastava, Garrison, and Brenner[57] in simulations using the Tersoff potential. However, in their simulations the adatoms deposited earlier first saturate the two dangling bonds of a dimer (the A sites in our notation in Sec. 3.3), then a third adatom breaks the dimer bond and inserts in it.[57] Our results suggest that such a mechanism is improbable at the low deposition rates used in epitaxy, since an adatom deposited in an A site will hop to an F site before the arrival of another adatom.[26]

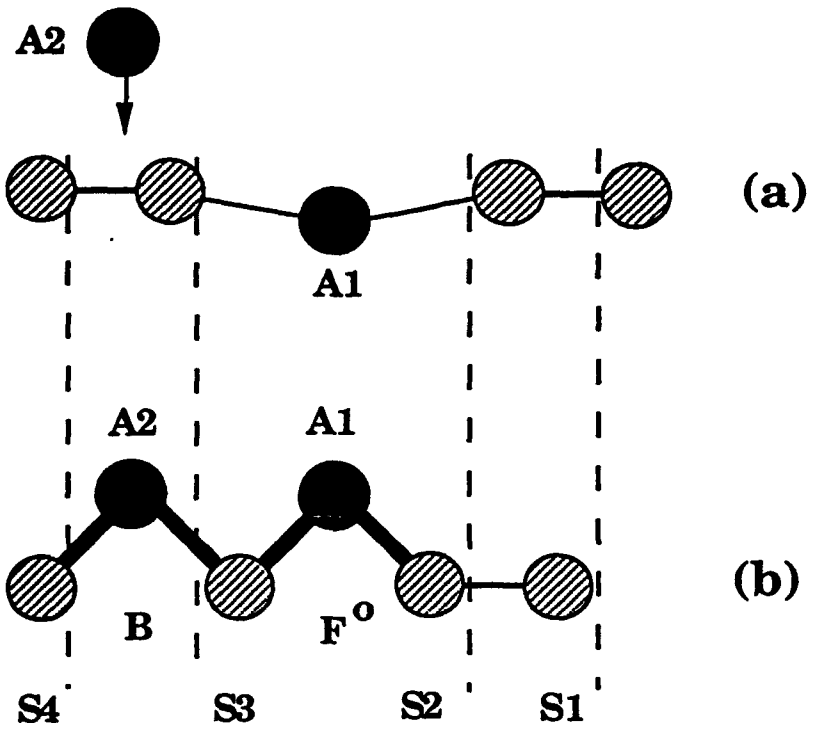

Fig. 4. Collective effect: The arrival of A2 helps A1 to take the position it will have when the layer is completed.

3.3. The Distribution of the Adsorption Sites

Next we deposit the Si atoms uniformly onto the unit cell of the reconstructed Si(100)-(2X1) surface. Our purpose is to determine all the adsorption sites, and the site occupation probabilities in the early stages of adsorption.[24]

At zero temperatures the adsorption sites are local potential energy minima. We deposit a particle on the surface and use an energy minimization program that moves the surface atoms and the adsorbed one until all the local minima are found. The same procedure is used to move the adsorbed atom from one adsorption site to another along the minimum energy path; this gives the energy barriers between the sites. The results are shown in Fig. 5 and Table

I. There are thirteen local minima within the surface unit cell, of which six, labelled A, B, C, D, E, and F, are distinct.[58] The others are equivalent, by symmetry, to one of the six. The reference energy for the binding energies at the local minima and the energy barriers separating them is that of the (2X1) surface with the adsorbate at infinity.

Now we examine the adsorption of the Si atoms on the surface sites described above. In these calculations an incident Si atom starts at the point (x, y, 3.5 Å) where the atom - surface interaction is zero. The x- and y-coordinates cover uniformly the unit cell defined by the rectangle $|x| \leq 1.0$ a, $|y| \leq 2.0$ a, where a=3.84 Å is the surface lattice constant before reconstruction (Fig. 5).

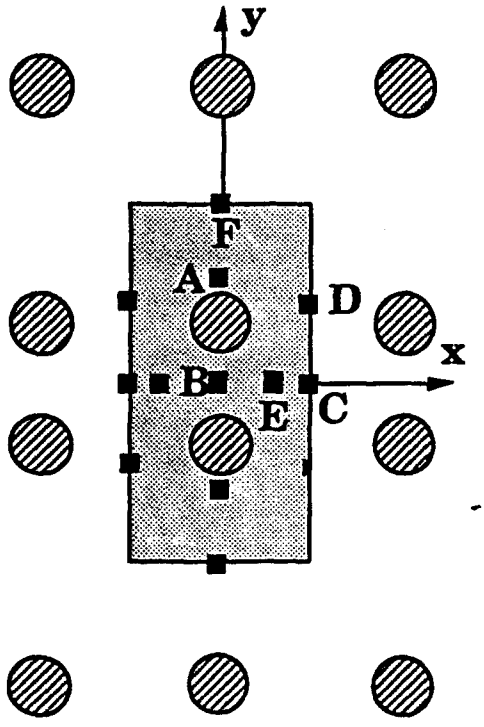

Fig. 5. The adsorption sites within the surface unit cell.

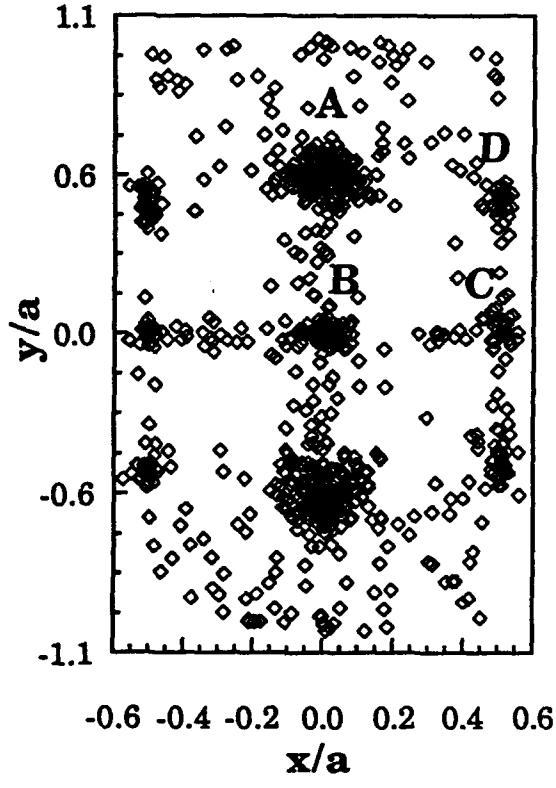

Fig. 6. A snapshot of 1000 adatoms at t ~ 0.9 ps.

Table I

The coordinates (x,y,z) of the binding sites, the binding energy E_b, and the barrier height V_b between two neighboring sites. s is the total area of a given type of adsorption site within the dotted rectangle in Fig. 5.

site	x (Å)	y (Å)	z (Å)	E_b(eV)	V_b (eV)		s (Å^2)
A	0.0	2.06	2.037	2.162	A → B	0.159	9.59
					A → F	0.323	
					A → D	0.200	
B	0.0	0.0	1.359	2.696	B → A	0.693	3.69
					B→ E	0.288	
C	1.92	0.0	1.508	2.639	C → D	0.176	1.10
					C → E	0.159	
D	1.92	1.73	1.704	2.635	D → C	0.190	8.66
					D→ A	0.692	
					D → F	0.759	
E	1.25	0.0	1.076	2.613	E → B	0.205	1.02
					E → C	0.133	
F	0.0	3.84	1.128	3.140	F→ A	1.301	5.90
					F→ F*	0.898	
					F→ D	1.245	

As one may expect, the atoms are drawn towards a few sites within the unit cell, even though the initial trajectories cover uniformly the whole area. What is perhaps unexpected is the population inversion observed in the earliest stages of adsorption: the incident atom is adsorbed with high probability at the sites A, B, C and D in Fig. 5, but not at the F site, even though the latter is the site

with the largest binding energy; the site A having the smallest binding energy attracts the largest fraction of the incident atoms.

In Fig. 6, we show a snapshot of the x and y coordinates of 1000 particles at 0.9 ps. It is clear that at this early time the trajectories have already clustered up around the sites A, B, C and D. By following the particles for a while longer we observe (see Fig 7) a slow depopulation of A accompanied by a population gain in B, which goes on for five picoseconds. This means that on this time scale the kinetic energy of some of the particles in A still exceeds the small energy barrier (0.159 eV) between A and B.

In Fig. 7 we show the time evolution of the fraction of trajectories whose x and y coordinates fall within the squares that define the adsorption sites A, B, C, and D. The initial population is proportional to the area associated with a given site (see the last column of Table I). After about 0.2 picoseconds the atom - surface interactions steer the incident particle towards the site A, away from F, D and E. Practically no particle manages to adsorb at F. The site occupation is pretty much established in about 0.6 ps, and the site A captures the largest fraction of particles.

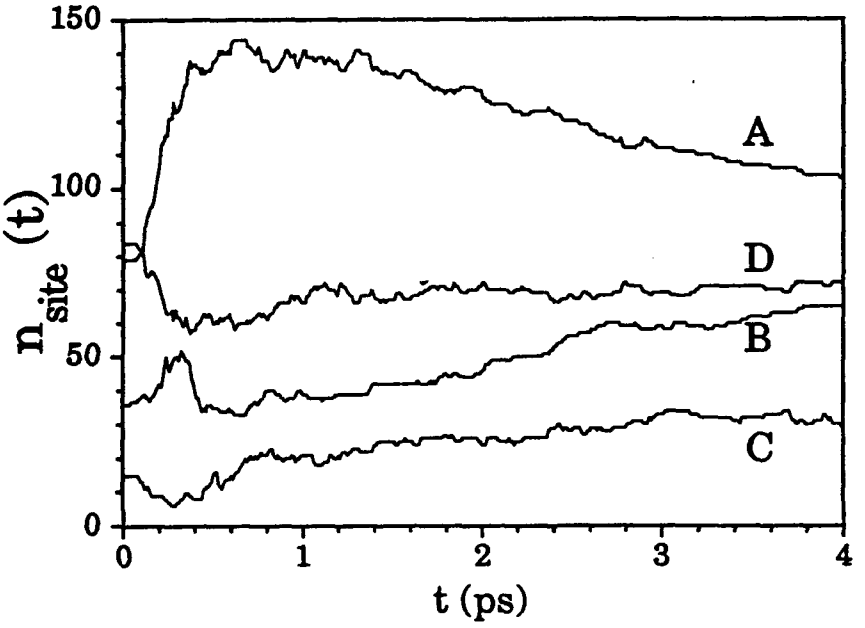

Fig. 7. The occupation of the surface sites at the early times of adsorption for 300 adatoms.

4. THE MIGRATION OF AN ISOLATED ADATOM ON THE SURFACE

4.1. The Site-to-Site Hopping Rates

At the temperatures of interest here the migration of an adsorbed atom on the surface takes place through thermally activated site to site jumps. The rates of such jumps can be crudely estimated by using the Arrhenius formula with a pre-exponential of 10^{13} sec^{-1} and the energy barriers given in Table I. Methods for exact calculations of the jumping rates are available[59,60] but will not be used here since our purpose is to gain a qualitative understanding of growth phenomena. In Fig. 8 we show the site to site hopping rates at T = 500 K, divided by the rate of the E → C jump.

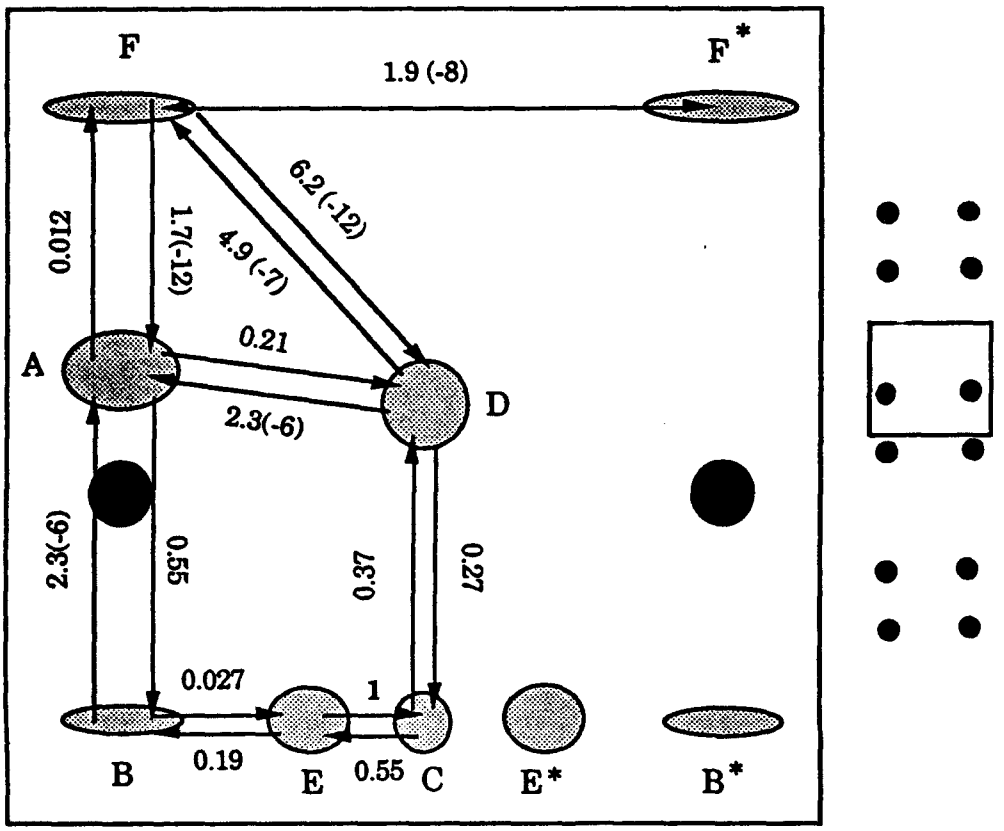

Fig. 8. The site to site hopping rates at 500 K.

The motion in the direction perpendicular to the dimer rows (i.e. B → A, D → F, F → A or F → D) is extremely slow. Furthermore, an atom adsorbed at B can move easily along the line B → E → C → E* → B* with likely side trips from C to D and back. Since there is essentially no fast pathway for an atom to exit the chain BEC(D)E*B*, the early motion after adsorption is practically one-dimensional. On a longer time scale the atom has a fair chance to jump into the site F where it will rest for a long time. On this time scale the sites F act as traps. At an even longer time scale the atom can move to F*, or, on the longest time scale, come back to D or A.

We note that the anisotropy of diffusion on Si(100) has been suggested by Lagally *et al.* to explain their STM results.[5,13] Lu and Metiu[9(b)] have argued that such anisotropy should be expected for all (100) faces of semiconductors having diamond or zincblende structures, since the barrier along the dimer rows is lowered by the fact that the breaking of the bonds to the initial site is concerted with the formation of bonds with the final site; no such lowering is present when the atom is moved in a direction perpendicular to the dimer rows and the energy barriers for that kind of displacement ought to be higher.

4.2. Diffusion on a Lattice with Many Sites

Most simulations of epitaxial growth have used models in which a particle jumps randomly on a square lattice. It is well known that for such a system the probability of finding the particle at a given site is described by a diffusion equation and the diffusion coefficient is proportional to the jumping rate. The temperature dependence of the diffusion coefficient is the same as that of the jumping rate and the latter is given by the Arrhenius formula. Our calculations suggest that reality is more complicated. On a short time scale the random motion takes place along a string with several sites and the particle can make side trips to the site D and back with a fairly high frequency.

If such motion is diffusional, the diffusion coefficient must

depend on all the site to site rate constants. Since the Arrhenius formula applies to the jumping rate, not to the diffusion coefficient, the relationship between the diffusion coefficient and the temperature can be rather complicated. If the relationship happens to be of an Arrhenius form, the activation energy and the pre-exponential will not have a simple meaning. On the time scale on which the atom is likely to be trapped into an F site the motion is not diffusional; i.e. the mean square displacement is not proportional to time.

To understand the nature of the adatom migration we have performed stochastic kinetic simulations to calculate the mean square displacements for three models: One in which both the side trips to D and the access to the traps are forbidden; one in which only the traps are inaccessible; and one in which all processes are allowed.[25]

The stochastic kinetic simulation moves a Si atom along the sites shown in Fig. 8 with probabilities proportional to the ratio between the rate constant of the appropriate jump and a reference rate k_r. We use for k_r the rate of the jump E→C at 600 °C, which is the fastest. The E→C jump is performed whenever attempted. The time $(k_r)^{-1}$ provides the time scale for the simulation. The time in the plots in this subsection is $k_r t$, where t is the clock time. The time unit $(k_r)^{-1}$ happens to be close to a picosecond. The averages are performed over 10^4 independent runs.

4.2.1. The Random Walk on the Fast String

To understand the migration process we examine first the random walk on the fast string ..BECE*B*.. when the jumps to A, D and F are forbidden. The highest barrier along this string is 0.29 eV (for B->E), and the lowest is 0.13 eV (for E->C). The time dependence of the mean square displacement $\langle x^2 \rangle$ obtained in the stochastic kinetic simulations at 400, 600, and 800 °C are shown in Fig. 9. The plots are linear in t, indicating that the motion is diffusional; the proportionality constant is twice the diffusion coefficient.[25]

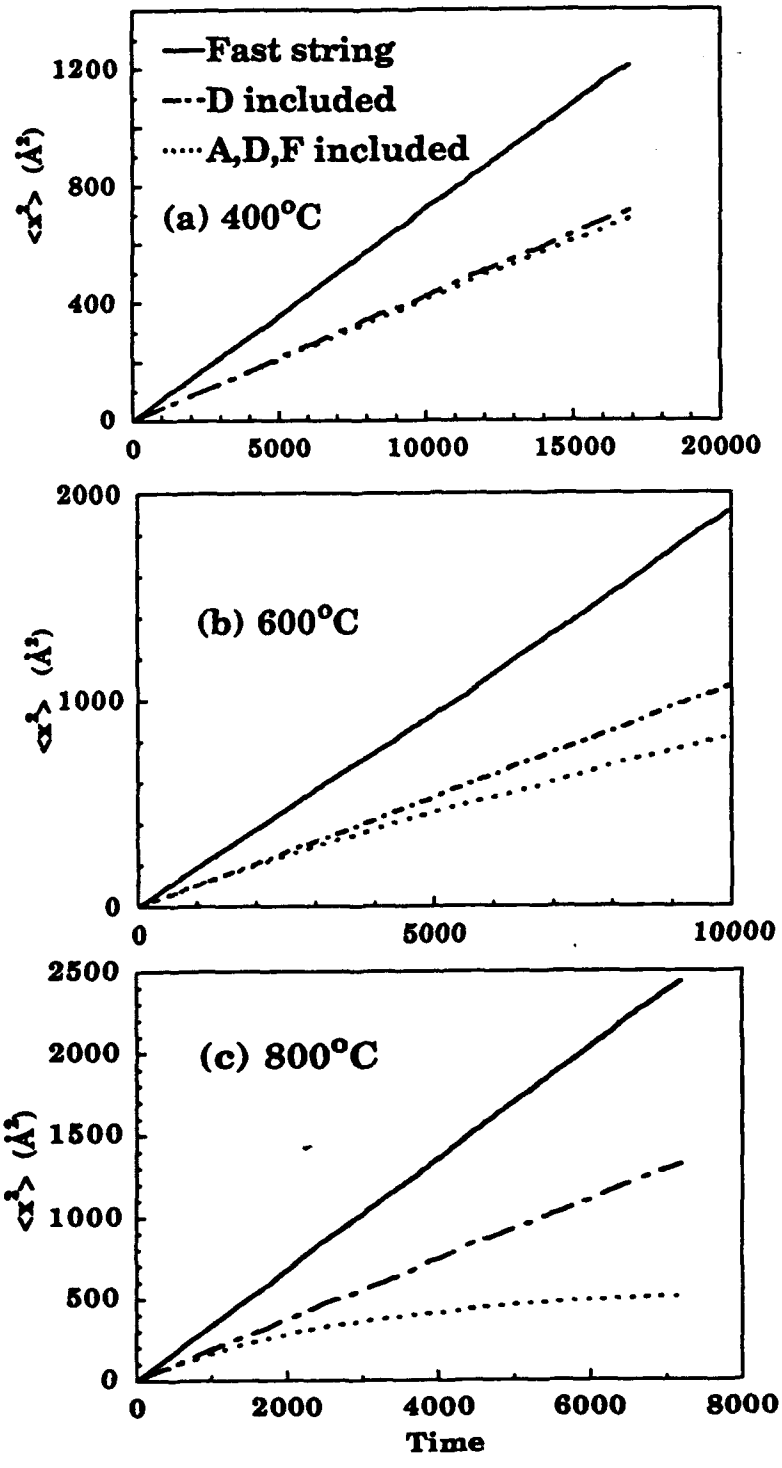

Fig. 9. Mean square displacements as a function of time at 400, 600 and 800 °C, for the three models.

The temperature dependence of the diffusion constants is plotted in Fig. 10, for a temperature range from 200 to 800 °C. This curve has an Arrhenius form with an activation energy of 0.24 eV and a pre-exponential of 2.36 $Å^2/\tau$. Here $\tau=(k_r)^{-1}$ and the reference rate k_r = $1.71x10^{12}$ sec^{-1}. We can define an effective jumping rate k_e by using $D_e= a^2 k_e$,where a is the B to B* distance. The pre-exponential A_e in the effective jumping rate k_e is $A_e = 2.36\ k_r/a^2 = 2.76x10^{11}$ sec^{-1}. We see here a "compensation effect": while all the rates in the model have pre-exponentials of 10^{13} sec^{-1} the pre-exponential of the effective rate is almost two orders of magnitude smaller. The activation energy of the diffusion coefficient is also smaller than that of the highest barrier along the fast string.

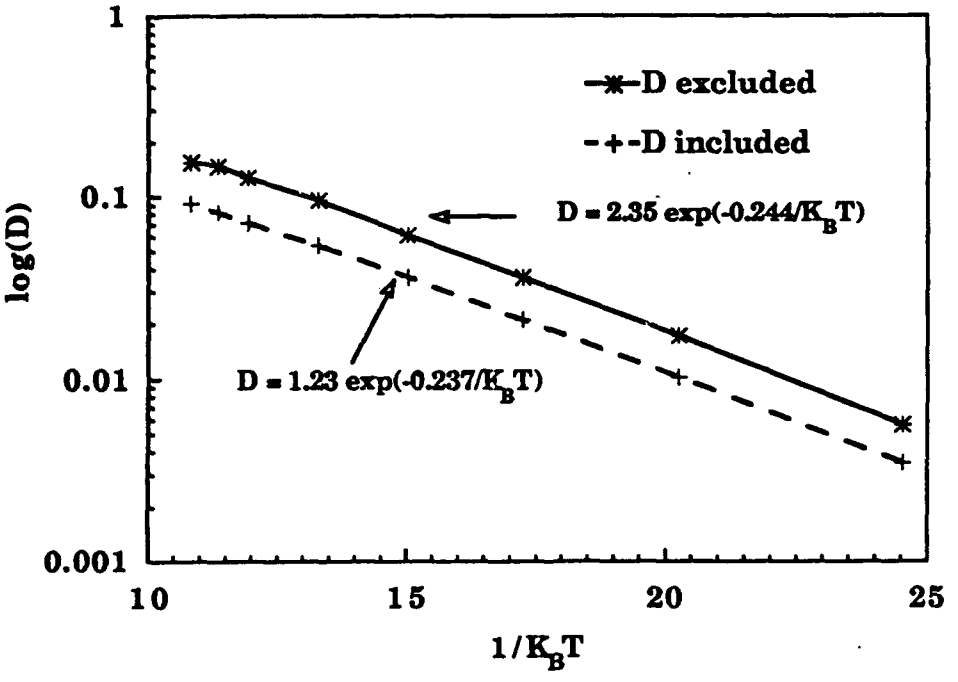

Fig. 10. Diffusion coefficient for two different models of multisite one-dimensional diffusion: without and with side trips, respectively.

To understand these results we have examined a simpler model in which an atom jumps along a string which has only two sites per unit cell (Fig. 11). The rate equation for this system is

$$\frac{dP_1(\alpha;t)}{dt} = k_{21}P_2(\alpha\text{-}1;t) + k_{21}P_2(\alpha;t) - 2\,k_{12}P_1(\alpha;t) \qquad (4.1a)$$

$$\frac{dP_2(\alpha;t)}{dt} = k_{12}P_1(\alpha+1;t) + k_{12}P_1(\alpha;t) - 2\,k_{21}P_2(\alpha;t)\,. \qquad (4.1b)$$

$P_i(\alpha;t)$ is the probability that the atom is at a site of type i (i=1 or 2) in cell α, at time t, and k_{ij} is the rate of the i→j jump.

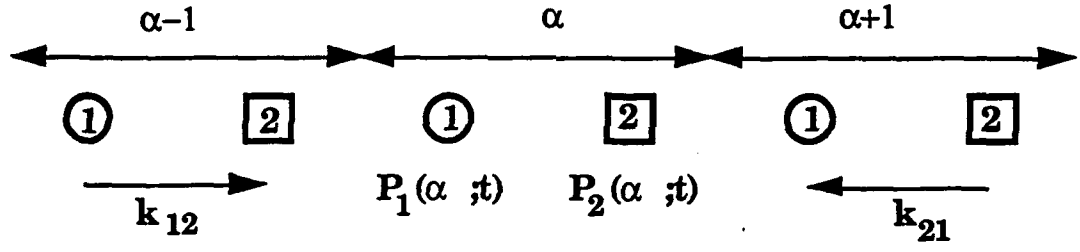

Fig. 11. A schematic representation of an one dimensional diffusion channel with two inequvalent sites.

A simple analysis[25] shows that the probability $P(\alpha;t)= P_1(\alpha;t)+P_2(\alpha;t)$ that the particle is in the cell α at time t, satisfies a diffusion equation with the diffusion constant

$$D = \frac{1}{2}\left\{\frac{k_{12}k_{21}}{k_{12}+k_{21}}\right\} a^2. \qquad (4.2)$$

Clearly the diffusion coefficient does not have a simple Arrhenius temperature dependence if each of the two rate constants

k_{12} and k_{21} does. Nevertheless, as seen in the simulations reported above the temperature dependence is often fitted well by the Arrhenius formula. To find the meaning of the pre-exponential and the activation energy in such fits we expand ln D in powers of $1/(k_B T)$:

$$\ln D = \ln \{ \frac{a^2}{2} (\frac{f_{12} f_{21}}{f_{12}+f_{21}}) \} - \{ \frac{v_{21} f_{12} + v_{12} f_{21}}{f_{12} + f_{21}} \} (\frac{1}{k_B T}) + \{ \frac{f_{12} f_{21} (v_{12} - v_{21})^2}{2 (f_{12}+ f_{21})^2} \} (\frac{1}{k_B T})^2 + O((\frac{1}{k_B T})^3) \qquad (4.3)$$

Here f_{ij} and v_{ij} are the pre-exponentials and the activation energies in the rate constants k_{ij}. The pre-exponential in the diffusion coefficient is $a^2 f_{12} f_{21} / [\, 2 (f_{12}+f_{21}) \,]$ and the activation energy is $(f_{12} v_{21} + f_{21} v_{12})/(f_{12}+f_{21})$. The Arrhenius formula is valid when the third term on the right hand side is negligible compared to the first two. Similar relationships exist for three and four site systems.[25]

4.2.2. Diffusion Along a String with a Side Trip

Qualitatively, it is not difficult to see that the side trips from the C to the D sites and back will delay the progress of the atom along the fast string, thus leading to a smaller diffusion coefficient. To find how important this effect is we performed stochastic kinetic simulations with a model in which these side trips are allowed, but the jumps to A and F are still forbidden. The time dependence of the mean square displacement along the fast string is shown in Fig. 9 for 400, 600, and 800 °C. The proportionality to t means that the motion is diffusional. The temperature dependence of the diffusion coefficient obtained from the mean square displacement satisfies the Arrhenius equation (see Fig. 10) and a fit of the results leads to

$$D(T) = 1.23 \exp\{ - \frac{0.24}{k_B T} \} \quad (\text{Å}^2 k_r) \qquad (4.4)$$

Allowing the side trips did not change the effective barrier, but

diminished the pre-exponential factor from 2.36 $Å^2 k_r$ to 1.23 $Å^2 k_r$.

The analysis of a simplified model of random jumps along a chain having two sites in the unit cell along the chain and one site for a side trip (see Fig. 12) gives the diffusion coefficient

$$D = \frac{a^2}{2}\left\{\frac{k_{12}k_{21}}{(k_{12}+k_{21}) + k_{12}k_{23}/k_{32}}\right\}. \qquad (4.5)$$

The definition of the rate constants k_{ij} is given in Fig. 12. Note that this equation is not valid if k_{32} becomes zero because in that case the site 3 acts as a trap and the motion is no longer diffusional. In the other extreme where k_{32} is very large or k_{23} is very small, this equation reproduces the diffusion coefficient for the chain without a side trip. A chain with a side trip is identical to a chain without a side trip in which the lifetime at the site from which the side trip originates is increased.

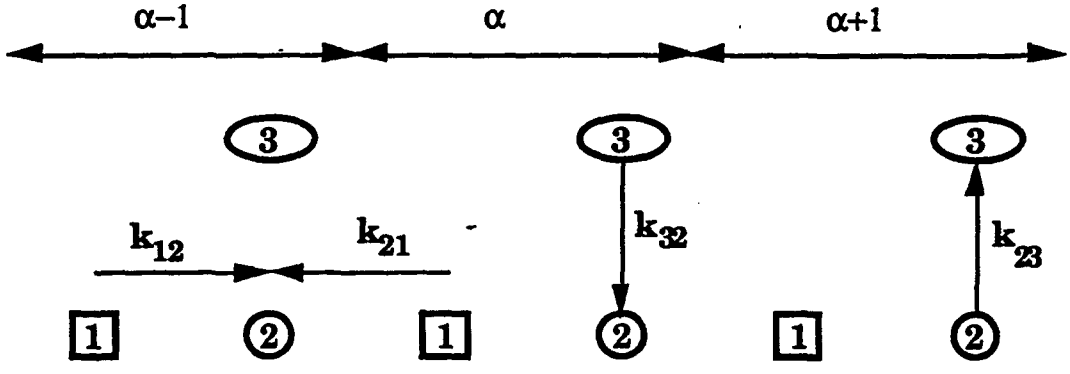

Fig. 12. A schematic representation of a model in which the particle can jump along an one dimensional lattice having two sites (the square and the circle) and it can also take a side trip from the site 2 to the site 3 (the ellipse).

4.2.3. Migration Along the Fast String with Side Trips and Traps

Now we present the results of simulations in which both the side trips and the traps are included. The time dependence of the mean square displacements $\langle x^2 \rangle$ is shown in Fig. 9. The curves for $\langle x^2 \rangle$ rise linearly at early times, then bend and flatten out at longer times. This happens because there is a small probability that a Si atom visiting the site D will jump to the site F and remain trapped there. When this happens the atom no longer contributes to the growth of $\langle x^2 \rangle$. The time dependence of the mean square displacement varies smoothly from linear to constant because different atoms are trapped at different times. At a time scale longer than the lifetime at the site F the visiting atom leaves the trap by a hop parallel to the dimer rows into another trap F*; the barrier for this move is 0.9 eV. The probability to hop back onto the fast string is rather small, with a barrier of 1.25 eV. The migration on this longer time scale is not investigated here.

Notice the mean migration distance at 800 °C is shorter than that at 600 °C. This happens because at the higher temperature the trapping rate is larger and the mean square displacement starts deviating from the linear behavior at an earlier time.

The observed behavior can be understood by examining diffusion along an one-dimensional string with a small probability that the particle leaves the string and gets trapped. To describe this system we must use a random walk equation with a rate term to jump into a trap, and no possibility of coming back. The mean square displacement $\langle x^2 \rangle$ for such a model is

$$\langle x^2 \rangle = \frac{2D}{s}\left(1 - e^{-st}\right) \qquad (4.6)$$

Here D is the diffusion coefficient on the string and s is the rate constant to fall in the trap. To test whether this equation describes well the behavior of $\langle x^2 \rangle$ observed in the simulation we calculate the mean square displacement for D = 0.07 $\text{Å}^2 k_r$, which is the diffusion constant of the one dimensional motion with side trips, and $s=10^{-4}$,

which is estimated from the rate of hopping from C to D and then D to F. The empty circles in Fig. 13 show the results given by Eq. (4.6) while the solid line shows the results of the simulation. The agreement is excellent.

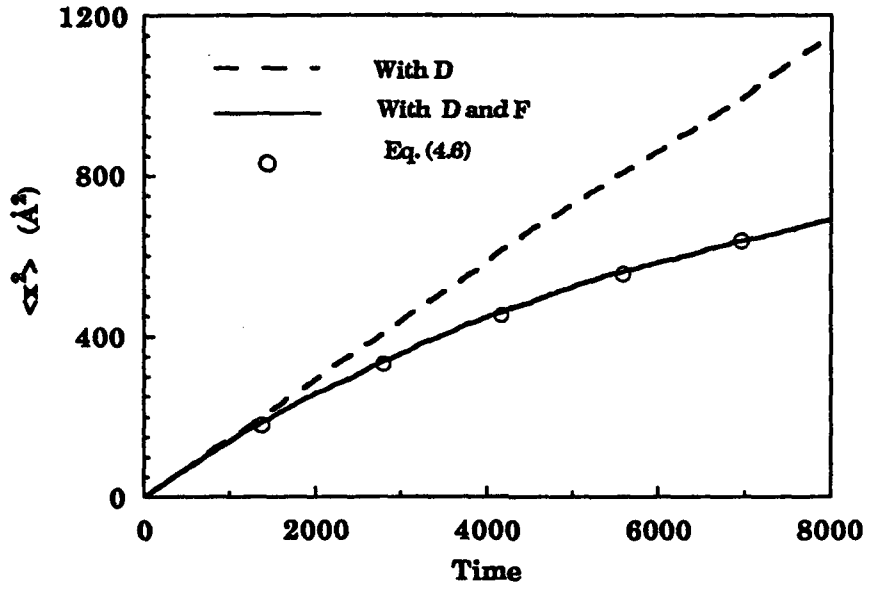

Fig. 13. Time dependence of the mean square displacement for the model allowing side trips to D and visits to F.

5. ADATOM-ADATOM INTÉRACTIONS AND THE PATHWAYS FOR DIMER STRING GROWTH

The STM measurements[16,17] show that at low coverage the silicon atoms adsorbed on the Si(100)-2X1 surface form string like islands perpendicular to the dimer rows on the surface. These island shapes are highly unusual. The reason why the silicon atoms prefer these shapes and the mechanism of their formation are not understood. The large number of strings indicates that many nucleation centers are produced in the early stage of the deposition. It is not clear what these nucleation centers are. Our studies reported in the previous section indicate that the F sites, located

between the substrate's dimer rows, are very slow to fill; the site to site jumps leading to them have low rates compared to those of the B sites. To form the strings observed by STM the migrating atoms fill as many F sites as B sites. This is rather surprising and requires an explanation. In particular we need to know why there are so few F site vacancies in the islands. Finally, the work reported in the previous section indicates that the diffusion of the single atoms on the surface is highly anisotropic. Since the strings are perpendicular to the direction of fast diffusion, most of the single atoms moving on the surface will reach the *side* of an existing string; given this, it is difficult to understand how the string is getting longer and not wider. Below we provide an answer to these questions.

In many surface science systems it is assumed, with good reason, that the diffusion coefficient at high coverage is not radically different from that of a single particle. The change caused by increased coverage is usually calculated by a mean field model in which the change depends on the mean coverage only. This is not true for silicon, for which the interactions are not only very strong but are also spatially directed. The rate to jump from site to site depends not only on the number of neighbors surrounding the sites[9-11] but also on their *precise location*. It is useful to think of the two dimensional clusters formed by the adsorbed atoms as distinct isomers: clusters with the same number of atoms have, in most cases, substantially different properties if their "structure" differs. The isomerization, dissociation and atom capture rates differ from isomer to isomer. To understand how the islands grow and change shape we must consider the properties of a very large number of clusters. We discuss here only those that provide the fastest steps[26] leading to the strings observed experimentally. The rates are estimated by calculating the energy barriers for each step and assuming that all rate constants have the same pre-exponential.

We consider configuration changes achieved by moving one atom from a site i, of the initial configuration to a site j of the final one. Occasionally, we have also investigated changes achieved by moving dimers, when our intuition suggested that they might be rapid; we have found dimer motion too slow to be an important factor in island growth. The potential energy barrier to go from a site S_i to

another site S_j is determined as follows. We first place the jumping atom at S_i. Then the atomic positions of all the atoms (the one whose motion is studied, the adsorbed atoms neighboring S_i and S_j, and the pertinent substrate atoms) are relaxed to minimize the total energy of the system. Next, we change the position of the atom whose migration we want to study, by a small displacement along the surface towards the final site, by changing, for example, its x coordinate. Then we keep x fixed at this new value and vary the coordinates of all the other atoms, as well as the y and z coordinates of the atom of interest, until we find the minimum energy. This procedure is repeated until the atom being displaced reaches the final site.

The interaction with the substrate and the neighboring atoms is so strong that it is not possible to describe the reaction path by specifying only the displacement of the jumping atom. As the jumping atom moves towards the final site, the other atoms can also undergo substantial displacements. There are in fact many pathways by which an atom goes from S_i to S_j, that differ through the way the other atoms are moving, and have different energy barriers. The one with the lowest barrier defines the preferred jumping path.

The substrate is modeled by a cluster of 495 atoms, distributed in five layers. Of these, 213 atoms are allowed to relax to give the lowest potential energy for the whole system; the rest are fixed and provide a template.[26]

At this point it is useful to remember that an atom landing on a Si(100)-2X1 surface moves rapidly along the dimer rows, and the rate to jump to an F site is low. Nevertheless, at the low deposition rates typical to epitaxial growth experiments, the atoms deposited earliest are likely to reach an F trap before having a chance to encounter another adsorbed atom. The most likely path to jump into an F site from the fast channel is via C→D→F, with barriers of 0.15 and 0.68 eV, respectively. The jump of an atom from an F site back on the fast string is very improbable. The F→F* jump also has a large barrier of 0.9 eV (see Fig. 8). For this reason we call the set of sites F, F*, etc. located between the substrate dimer rows, the slow string.

Atoms deposited later move along the fast strings and either fall

into unoccupied F sites or bind to the occupied ones forming pairs, with one atom in F and the other in B (Fig. 14(b)) or in E (Fig. 14(c)). The pairs are easily formed: the highest barrier for the move from B' to B (Fig. 14(a)) is 0.24 eV. Once formed, they are fairly persistent: the atom at F will not move, and the barrier to move from E to E' (see Fig. 14(c)) is $V_{E->E'}$ = 0.73 eV. Thus, an atom at F pins down an atom running along the nearby fast string localizing it in either the B or the E site nearby; the barriers $V_{E->B}$ = 0.23 eV and $V_{B->E}$ = 0.20 eV are low and the atom jumps back and forth between B and E. Therefore, the nucleation centers for the strings are the early atoms which reach the F sites. There are many such nucleation centers because the deposition rate is very low and this gives the early atoms a chance to reach the F sites, get stuck there and trap another atom running along the fast strings.

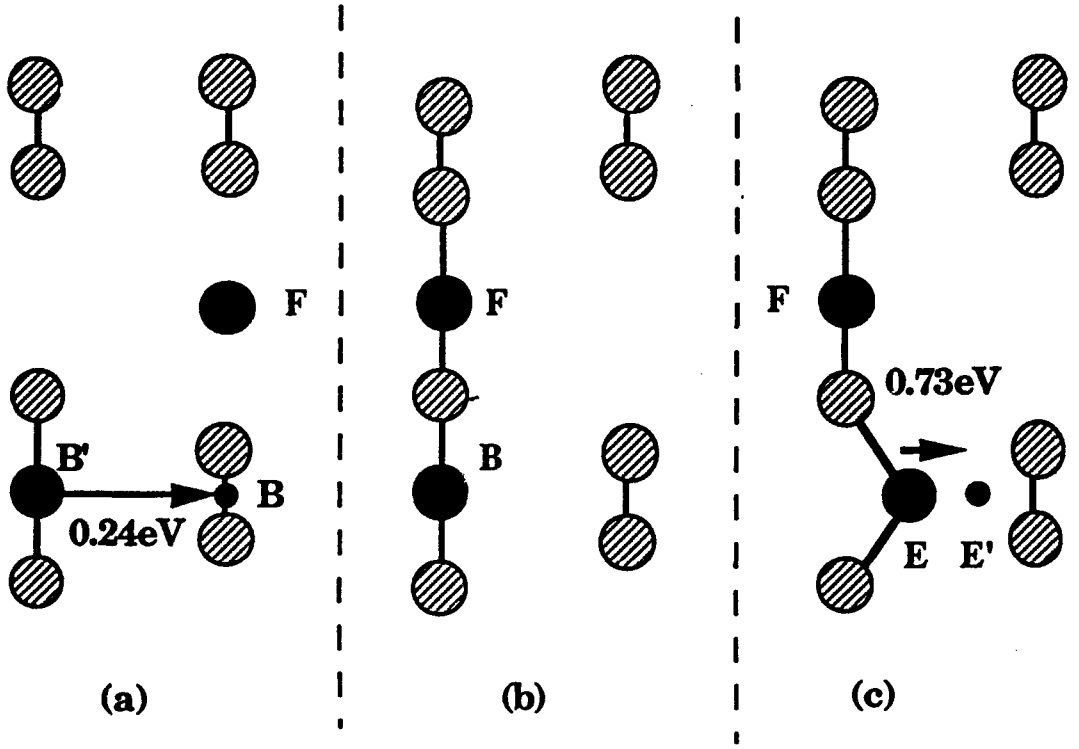

Fig. 14. An adatom trapped in the site F pins down an atom running on the nearby fast string.

We have also examined the mobility of a dimer located on the fast or the slow string to see if dimer diffusion plays an important role in the growth process. We find that once a dimer is formed it is essentially immobile.

As more atoms are deposited on the surface they move rapidly along the dimer rows to form the triplets shown in Fig. 15. In Fig. 15(a), the three atoms shown are located at sites corresponding to the growth pattern observed in STM. The atoms at B_1 and B_2 form a stable dimer. The presence of atoms at B_1 and B_2 reduces the barrier for the trapped atom to move from F_1 to F_2 but it will not break away from the trimer. In Fig. 15(b), the two atoms located at the sites E_1 and E_2 are in the wrong place (i.e. not where observed experimentally, in the final structure).

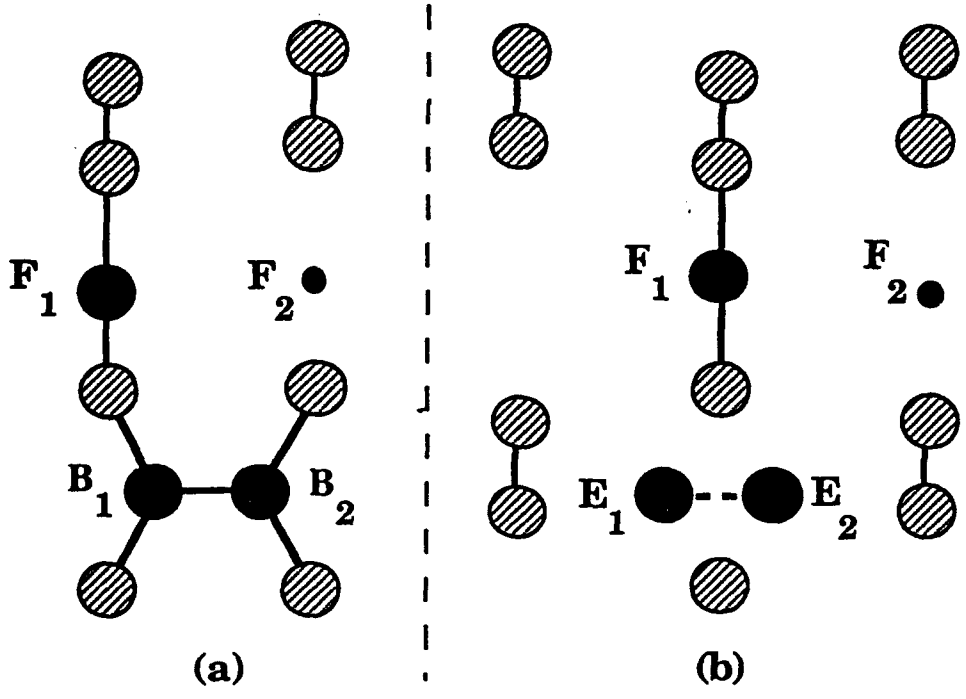

Fig. 15. The formation of triplets: (a) is stable, (b) is a precursor state for the process shown in Fig. 16.

It turns out that the wrong configuration shown in Fig. 15(b) is an important precursor state for the occupation of F_2 and the formation of a dimer in the slow string. The process is shown in Fig. 16. If we pull the atom 2 in Fig. 16(a) as indicated by the arrow, the atom 1 will follow for a while; then, the 1-2 bond breaks and 2 ends at an F site (F_2 in Fig. 16(b)) and 1 in an E site (E_2 in Fig. 16(b)). The barrier for this move is 0.59 eV. This barrier is lower than the maximum barrier of 0.76 eV for the single atom C $\rightarrow$ D $\rightarrow$ F hopping, partly because as the atom 2 breaks the 1 - 2 bond and leaves the atom 1 behind, it forms a new bond with the atom at F_1.

Since in the low coverage limit the rate to reach the F sites is very small, many such sites will be left vacant unless the presence of other particles help fill the F sites. The move shown in Fig. 16 is important not only because it repairs an error (i.e allows the pair located at the wrong sites E_1 and E_2 to move to correct sites) but also because it provides a mechanism for populating a site F and form a stable dimer there.

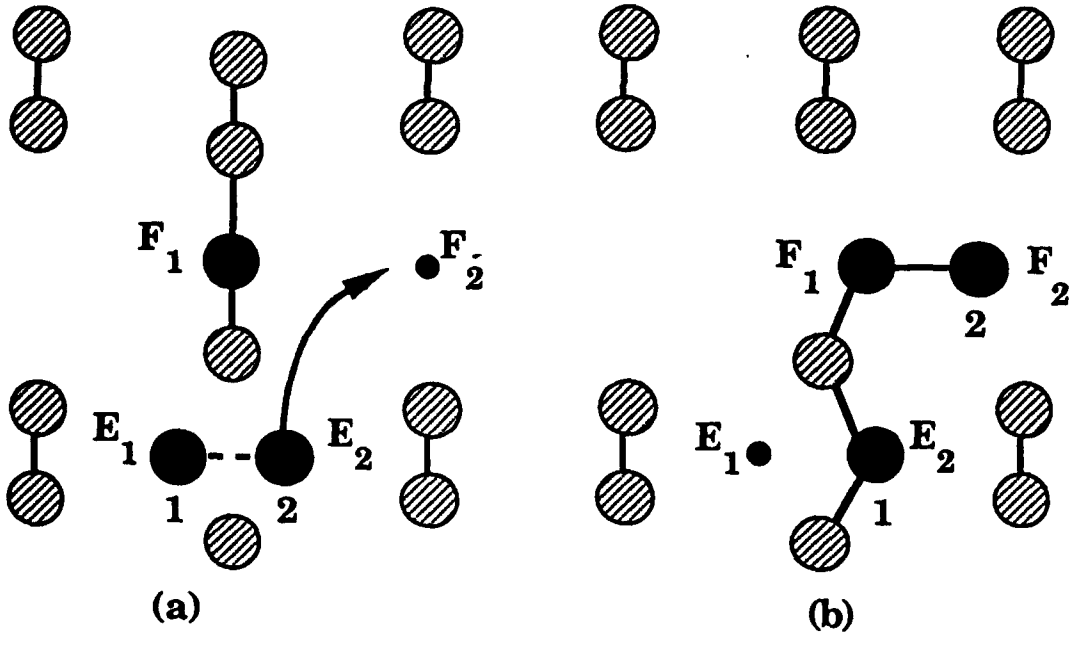

Fig. 16. A mechanism for the occupation of F_2.

If a fourth atom is brought close to the triplet configuration shown in Fig. 15(a), we find two other moves that can efficiently populate the F site (Fig. 17). In Fig. 17(a) the atom at E can easily jump into the site F_2 and form a dimer with the atom at F_1 (Fig. 17(b)). The highest barrier along this path is 0.44 eV. An adatom at C (Fig. 17(c)) can also hop into F_2 and form a dimer with F_1 (Fig. 17(b)); the barrier for this hop is 0.57 eV.

The jumps discussed above provide a kinetic pathways for the growth of a dimer string of length two (Fig. 17(b)). All other jumps that we have tried are too slow to alter this pathway significantly. This very short string can be considered a nucleus for the growth of a longer string. We investigate next how this growth takes place. To begin with, this small cluster will trap atoms moving on the fast string, at the sites B_3 and B_4. Further growth of the string takes place by filling the F sites at the end of this "nucleus" by one of the mechanisms discussed above.

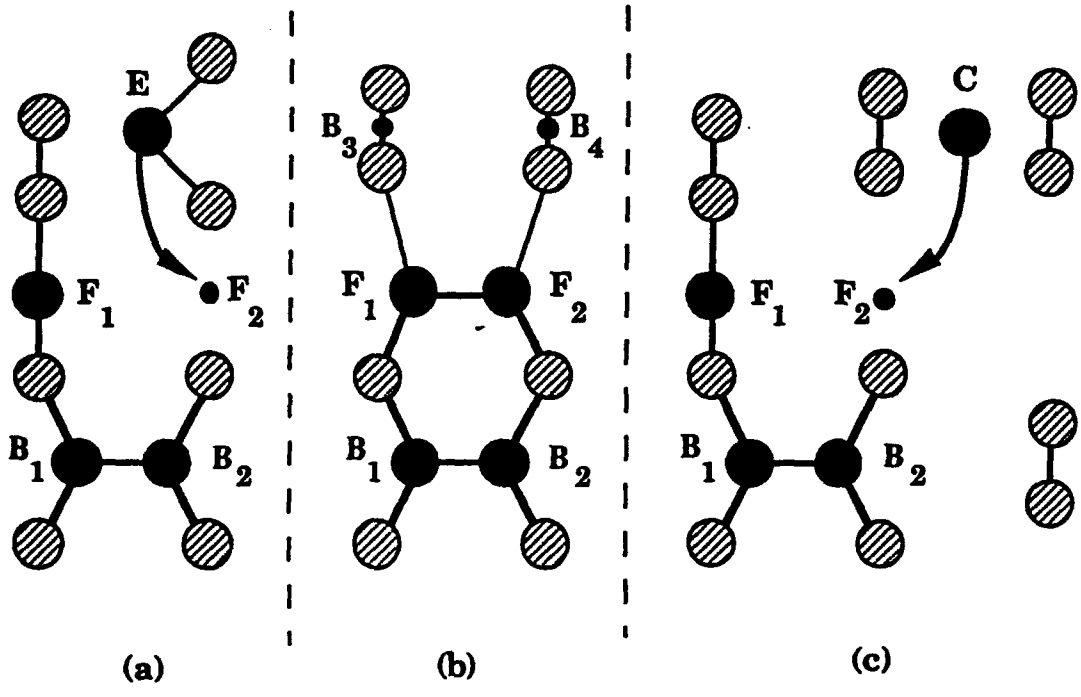

Fig. 17. (a) and (c) show two more mechanisms by which the F sites are populated. Both moves lead to the configuration (b).

We must now address what is perhaps the most puzzling feature of the observed growth patterns. The string grows in the direction perpendicular to the dimer rows, even though the free atoms moving along the surface move along the dimer rows and reach the string *on its side*. This should lead to a string widening rather than elongation. Therefore we must find a mechanism for the transport of atoms from the side to the end of the string.

We have examined two possibilities. Mo *et al.*[17] suggested that perhaps the probability that an atom sticks at the side of the string is much smaller than that for sticking at the end. Our energy calculations show that atoms reaching the end of a string are tightly bound there. The binding is much stronger if the string ends with an F site than with a B site. This is in agreement with the suggestion by Mo *et al.*[17] But, an atom can easily reach the side of the string (e.g. the atom 1 in Fig. 18(a)) and is *strongly* bound there. The energy barrier to jump away from the string is about 2 eV. This is contrary to the assumption made by Mo *et al.*[17]

The other possibility that we examined is related to recent work by Lu, Petroff and Metiu,[6] who have shown that a square lattice model with anisotropic interactions between the adsorbed particles leads to the formation of elongated islands. In their model these interactions facilitate the migration along the side of the string: particles reaching the side of the string move along it until they reach the head and get stuck there. The present calculations do not support this mechanism. The barrier to go from 1 to S in Fig. 18(a) is 0.362 eV, but the barrier from S to 1' is too high (2.557 eV).

There is a mechanism for transporting a particle from the side of a string to its end, and it turns out to be rather surprising. If we push the atom 1 (Fig. 18(a)) towards the string, 1 will replace the atom 2 and 2 will climb on the string and form a trimer. A side view of this trimer is shown in Fig. 18(b). Once placed by this exchange mechanism on top of the dimer string, atom 2 travels rapidly along the string and descends from it at the end, as shown in Fig. 19(a). If the string has an F site vacancy along the way, the atom 2 will repair it as shown in Fig. 19(b). Thus the exchange mechanism answers two of the questions posed at the beginning of this section: it transports the atoms from the side of the string to its end, if the string

is perfect, and it fills the vacancies if the string is defective.

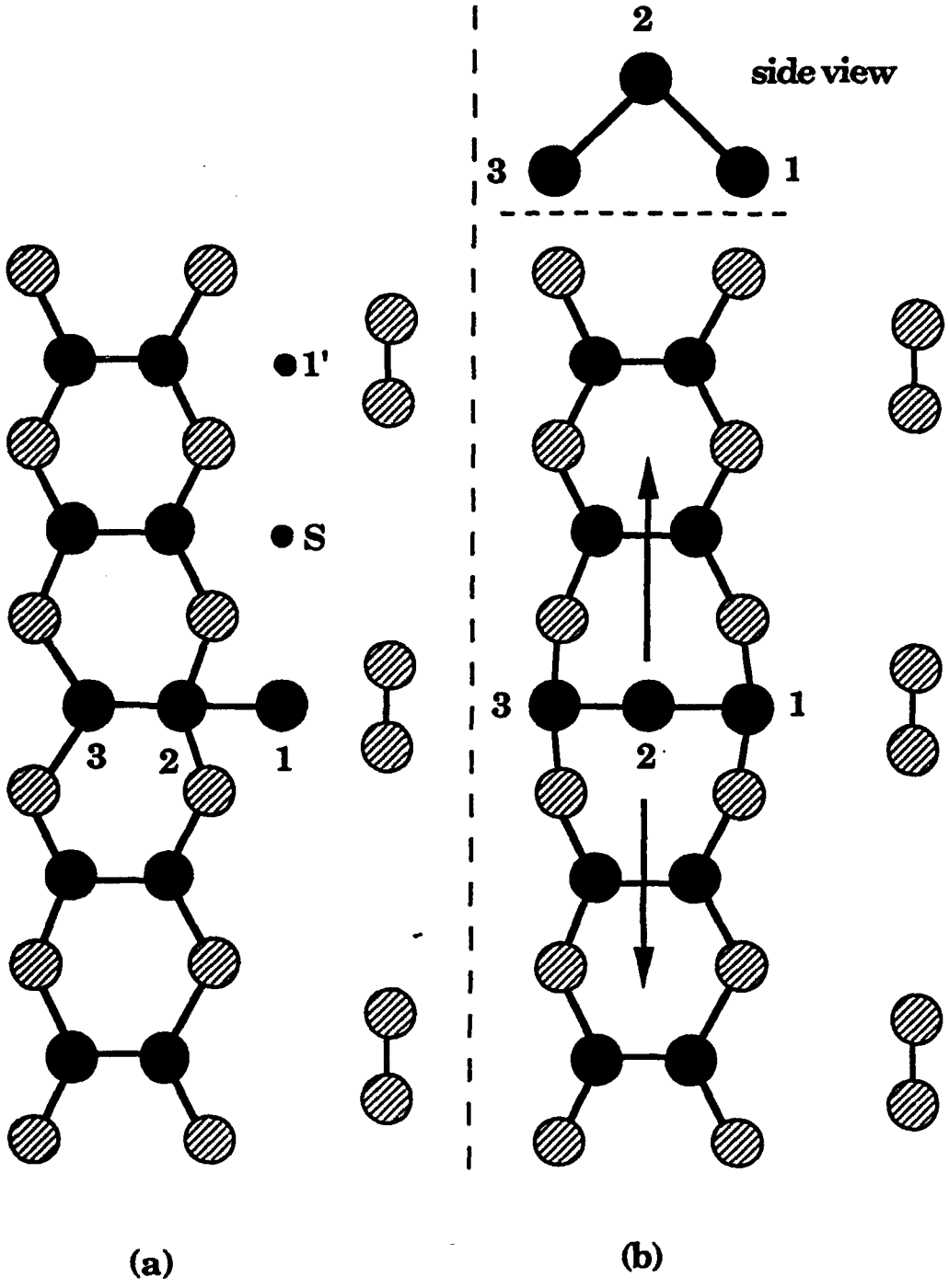

Fig. 18. The exchange mechanism that can put an atom on top of a dimer row.

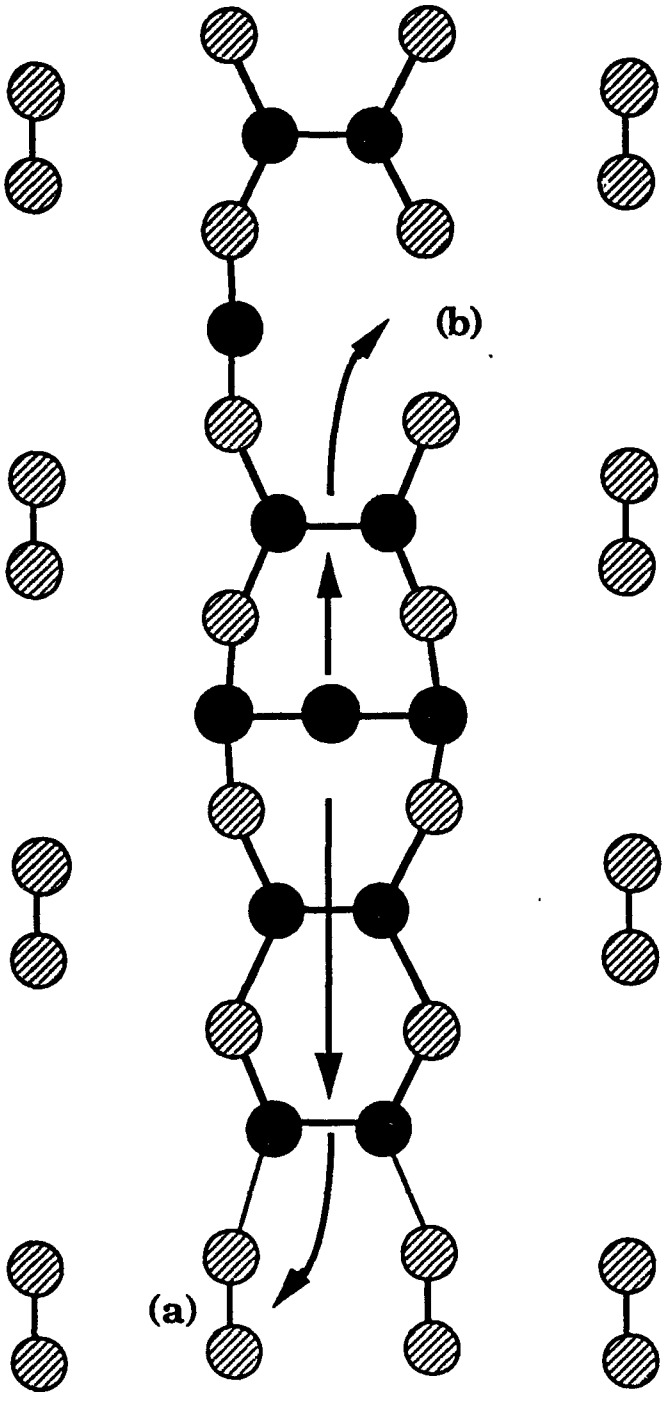

Fig. 19. An adatom on top of a dimer row can either (a) increase the length of the dimer row, or (b) repair a vacancy along it.

The exchange process takes place with a barrier of 1.07 eV, if the atom 1 is located as shown in Fig. 18(a), or with a barrier of 1.36 eV if atom 1 starts from the site S. Both these barriers are rather high and the exchange is not very efficient. Fortunately, the exchange rate is increased if a second adatom N approaches the adatom 1 located at the side of the string (Fig. 20(a)). They form an 1 - N dimer whose configuration is shown in Fig. 20(b). If the atom N in Fig. 20(b) is pushed towards the string the atom 1 will engage in the exchange process; the outcome is shown in Fig. 20(c). The presence of N lowers the barrier for the exchange process from 1.07 eV to 0.51 eV.

The exchange process is not the only option available to the 1 - N dimer shown in Fig. 20(b). It can also move away from the string by breaking the weak 4-1 bond, to reach the configuration shown in Fig. 20(d). The barrier for this move is 0.34 eV. The 1 - N dimer will be a nucleation center for the growth of a new dimer row adjacent to the first. Strings consisting of double and triple dimer rows have been observed experimentally. Their relative frequency depends on the growth conditions.

These findings provide the following description of the most likely pathway for string growth and error repair. Single atoms moving along the dimer rows of the substrate have no trouble reaching the side of an existing string. They will stick to it and are unlikely to jump away or to move along the side. There is a reasonable probability that through the exchange process the atom incorporates itself in the string, and lifts one of the string's atoms on top of it. Once on top the atom moves rapidly along the string; if it encounters a vacancy it falls in it and repairs it; if not, it reaches the end of the string, steps down from it and attach itself to the string increasing its length. Another likely scenario is that the atom stuck at the side of a string might wait there until another atom approaches it. The presence of the second atom aids the exchange process; however they may also decide to move jointly away from the string and form an adjacent dimer string.

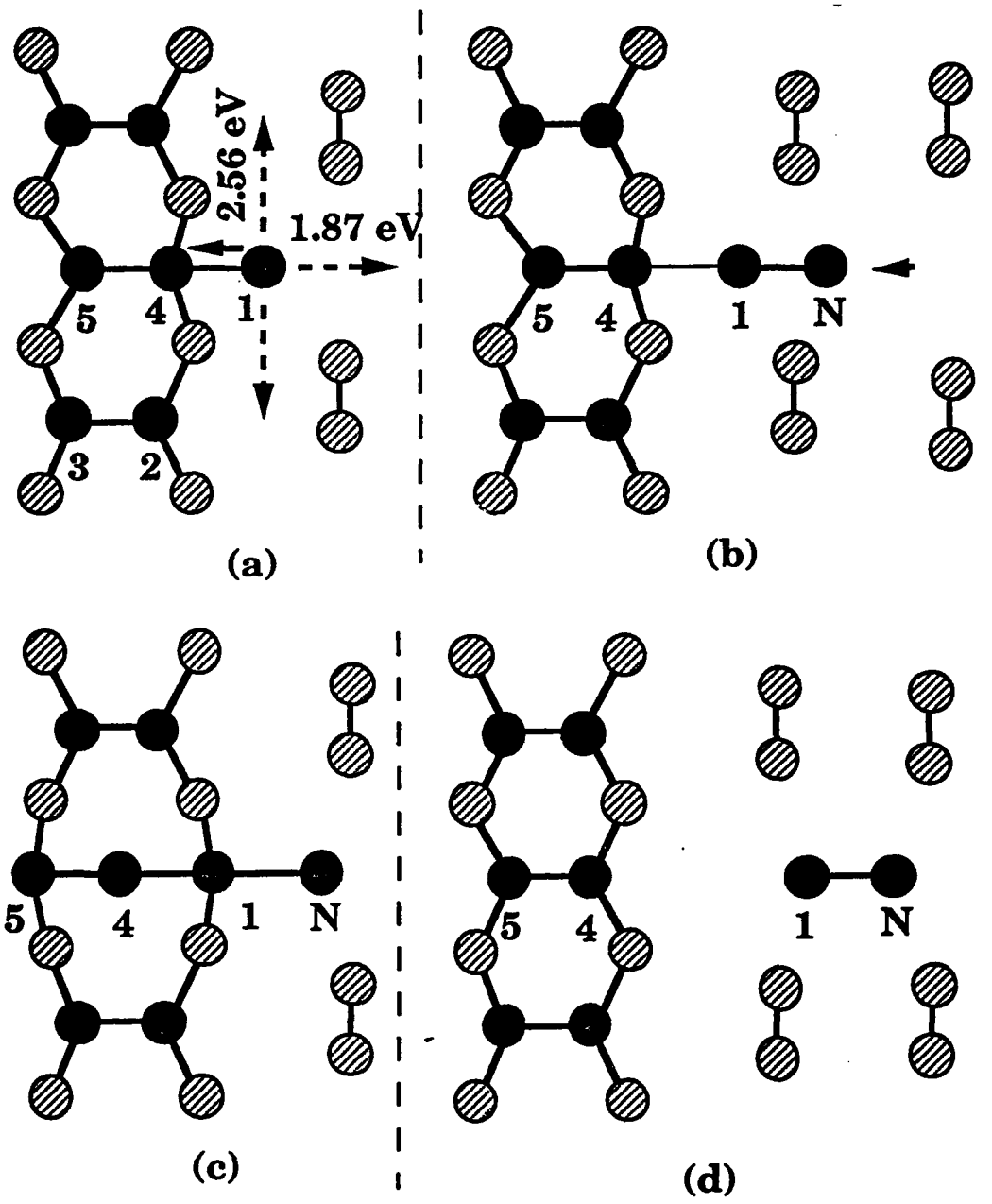

Fig. 20. (a) An adatom at the side of a dimer row before engaging in the exchange process. (b) The position N of a second atom, which helps 1 engage in the exchange process. (c) The atom 1 starting in the position shown in (b) undergoes an exchange process, and put the atom 4 on top of the dimer row. (d) The two atoms can move to create a nucleation center for the growth of a second dimer row.

6. ADATOM MOTION NEAR STEPS AND SINGLE TO DOUBLE STEP TRANSITIONS

Before discussing kinetics on stepped Si(100)-2X1 terraces we define some nomenclature which is best understood by looking at Fig. 21. This shows a stepped surface with *one-atom-high* steps. Such a surface has two kinds of terraces: a TA terrace, on which the dimer rows are perpendicular to the adjacent steps, and a TB terrace on which the rows are parallel. The TA and TB terraces alternate. A step having a TA terrace above it is called an SA step; one having a TB terrace above it is an SB step.[34]

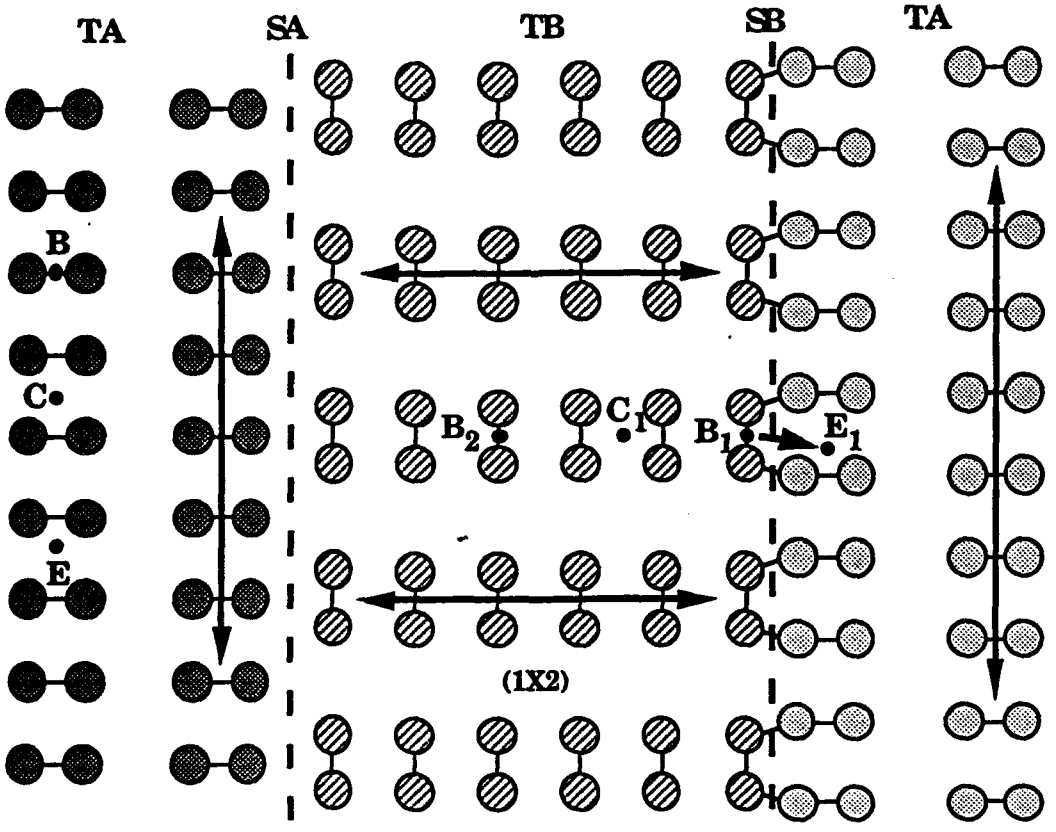

Fig. 21. A vicinal surface with one-atom-high steps. The down stairs direction is from the left to the right. The arrows show the fast pathways of adatom migration on the terraces.

On surfaces having *two atom high* steps, the dimer rows on all terraces are in the same direction. The terraces with the dimer rows perpendicular to the steps (called TB terraces) are more stable than the ones having dimer rows parallel to the steps (TA terraces). The steps separating the TB terraces are called DB steps.[34]

An interesting experiment was performed by Hoeven *et al.*,[3] who deposited half a monolayer of silicon on a Si(100)-2X1 surface having S steps and examined the result by STM. They found that after the deposition the surface had DB steps, with the dimer rows perpendicular to the steps (TB terraces). The width of these terraces is twice the width of the single atom high terraces of the initial surface.

The ability of the adsorbed atoms to create such a highly organized structure by undergoing uncorrelated, independent random jumps is rather striking. In this section we look for the kinetic pathway by which this transformation takes place. As a byproduct we also find a possible explanation for the reason why the SB steps are much rougher than the SA ones.[27]

The overall idea is rather simple. The experiment of Hoeven *et al.* [3] starts by the deposition of half a monolayer of Si atoms on a surface on which TA and TB terraces alternate (Fig. 22(a)). To build the double layer structure shown in Fig. 22(b) the deposited atoms must migrate in a peculiar way: the ones that have landed on a TA terrace must stay there; the ones that have landed on a TB terrace must move onto the neighboring TA terraces by either climbing up an SA step or down an SB step (Fig. 22(c)). When half a monolayer has been deposited the TA terraces will be completely covered. The length of the double terraces formed in this way is twice the length of the initial single terraces.

This simple model makes predictions that can be tested experimentally. For example, if a quarter of a monolayer is deposited the surface will consist of single atom high terraces; the length of the TB terraces will be roughly equal to 3L/2, while that of the TA terraces is L/2. Here L is the length of the starting terraces.

We proceed now to find if the mechanism proposed above is

substantiated by a more detailed study. To do this we determine the binding sites at the step and at the terrace edge, compute the energy barriers for the site to site jumps and use them to estimate the jumping rate constants. Then, we determine how the deposited atoms migrate to form double height terraces by assuming that they execute most often the jumps having the highest rates.

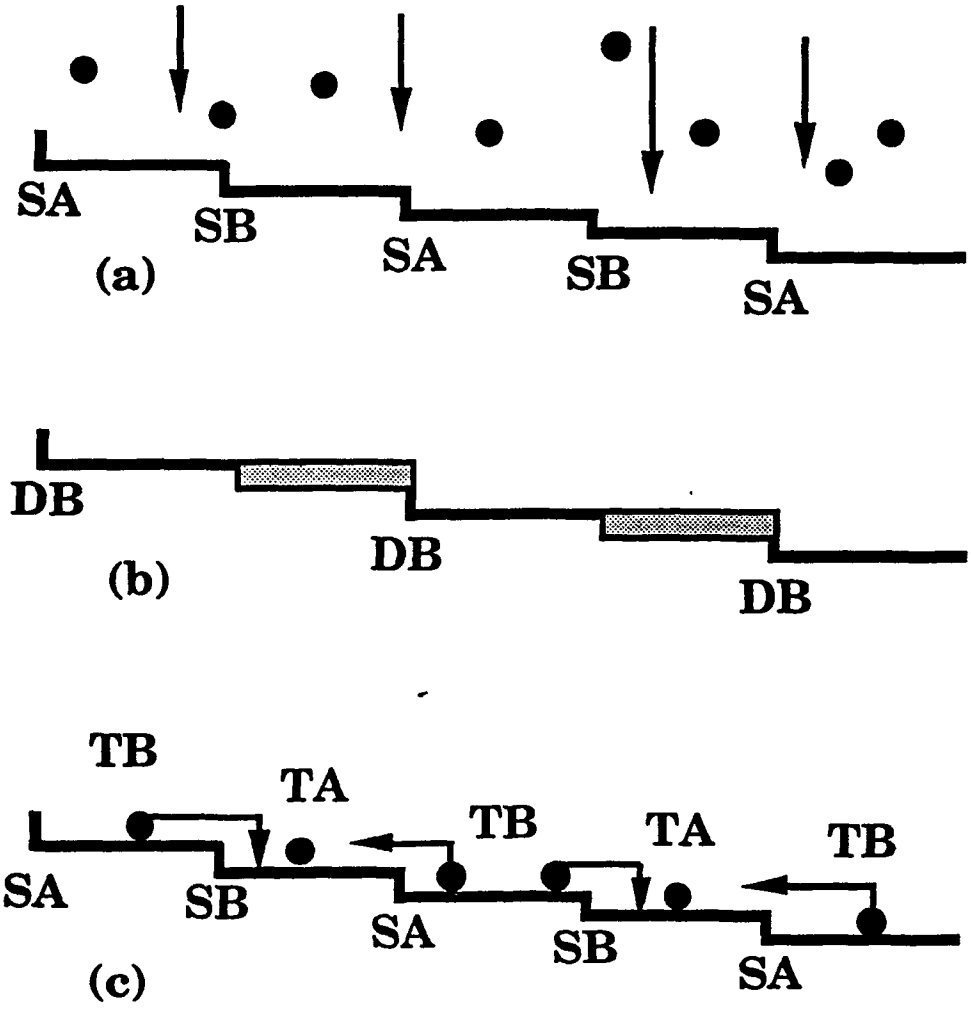

Fig. 22. A schematic representation of the kinetic mechanism for the transformation of single-atom-high steps into two-atom-high steps.

We examine now the steps invoked by the above mechanism for the double atom step formation. First we look at the motion across the TA terrace. According to the above mechanism this must be slow so that the atoms that land on TA will have a high probability to be stuck there. This is exactly what we find. We have already shown in the previous sections that an adatom will jump mainly along a dimer row, as indicated by the solid arrows in Fig. 21. Since an atom moving along the dimer row is likely to occupy the site B, E, or C, we have placed an atom at each of these sites respectively and moved it towards the step. The fastest pathway we found for moving across the TA terrace encounters a barrier of 1.25 eV.[28] This is higher than other relevant barriers and most of the atoms landing on the TA terrace will stay on it and form islands, just as assumed in the mechanism proposed above.

We must now see if we can find a rapid pathway for the migration of an atom from the TB terrace across the bordering steps and onto the neighboring TA terraces. We discuss first the motion across the SB step (Fig. 21).

Since on a TB terrace the dimer rows are perpendicular to the steps, the adsorbed atom has no difficulty migrating along the dimer row and reaching the SB step. The only possible difficulty may be the last jump, from the C_1 site to the site B_1 on the dimer nearest to the step (see Fig. 21). We find that the largest barrier encountered by an atom moving from C_1 to B_1 is 0.44 eV. This is substantially larger than the 0.29 eV barrier encountered by an atom moving from say C_1 to B_2 but it will not provide a substantial kinetic handicap. The terrace is very narrow and an atom that did not succeed going from C_1 to B_1 has many chances to try again.

An atom that has reached the C_1 site can descend across the SB step onto the TA terrace and reach the site E_1 (Fig. 21); to do this it must overcome two barriers, one of 0.40 eV and the other of 0.84 eV. Once at E_1, it can no longer leave the step edge: the barriers for moving back across the SB step on the TB terrace or away from E_1 on the TA terrace, are both of about 2 eV. This result is consistent with the experimental observation of Mo and Lagally,[5] who found that the SB step traps the adsorbed particles very efficiently.

On the other hand, the atom bound at E_1 can easily move along the SB step. The largest barrier encountered along the way is 0.37 eV. This is expected since the pathway along the step is on top of a dimer row, where the mobility is rather high. Thus, an atom descending from a TB terrace across the SB step to the E_1 site will move along the step until it encounters another adatom on the same string and form a dimer. This dimer will line up with the dimer row of the TB terrace, leading thus to the SB step roughening, and the TB terrace growth.

The descent of an isolated atom from a B_1 site to E_1 is rather slow. The rate of this transition is however greatly increased by the presence of another atom on the TA terrace near the step. One example is shown in Fig. 23(a) where an atom at E_1 helps the atom at a neighboring B_1 site to jump down across the step. The two atoms move to form a misaligned dimer (Fig. 23(b)) which later takes the correct position (Fig. 23(c)) by rotating by 90 degrees. The highest barrier in this sequence is 0.73 eV.

Next we examine how an atom on a TB terrace approaches the SA step bordering and climbs up across it to go on the adjacent TA terrace. Such an atom, denoted 1 in Fig. 24(a), reaches the position G without difficulty, by moving on top of a dimer row as indicated by the arrow. Once there, the atom is prevented by a barrier of over 2 eV from moving back onto the TB terrace. The barrier for moving along the SA step to the S site is 0.36 eV. Once there the atom is trapped. Before hopping to S the atom has a chance to participate in an exchange process. The outcome of this process is shown in Fig. 24(b): the atom 1 replaces the atom 2, and the latter is lifted up on the TA terrace. This exchange process must overcome an energy barrier of 1.07 eV. The rate is increased greatly if another adatom, denoted N in Fig. 24(c), is located nearby. The precursor configuration for the exchange is shown in Fig. 24(d). If we push the atom N towards the step the atom 1 will engage in an exchange process whose outcome is shown in Fig. 24(e). The presence of N lowers the barrier for the exchange process from 1.07 eV to 0.51 eV.

The atom placed by the exchange process on top of the dimer row (on the TA terrace) can easily move in a direction parallel to the step,

leaving behind the atom N in the configuration shown in Fig. 24(a).

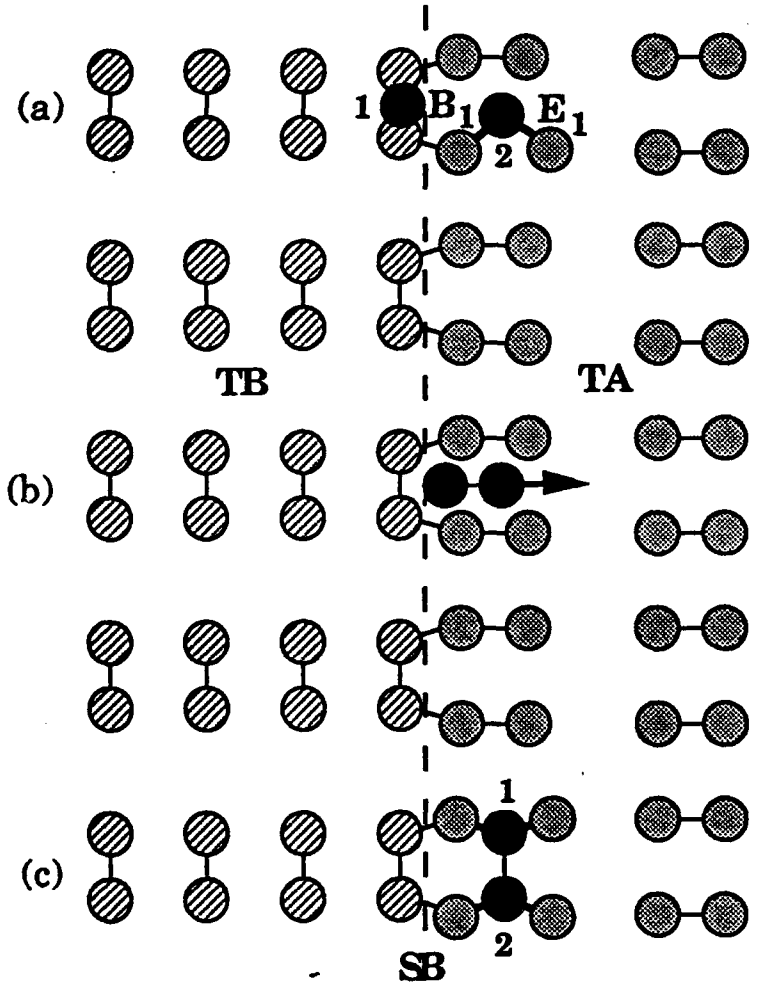

Fig. 23. The manner in which the migration of the atom 1 across the SB step is aided by the presence of the atom 2 near the step (on the lower terrace).

The exchange process is not the only possible move taking place from the configuration shown in Fig. 24(d): the atom N can break the weak 1-N bond and move away onto the TB terrace. The barrier for this is 0.9 eV.

Overall, the SA step is less effective than the SB step in trapping

the adatoms reaching it from the lower terrace. This is consistent with the observation of Mo and Lagally[13] that more islands are formed on a TA terrace near the SA step than on the TB terrace near the SA step.

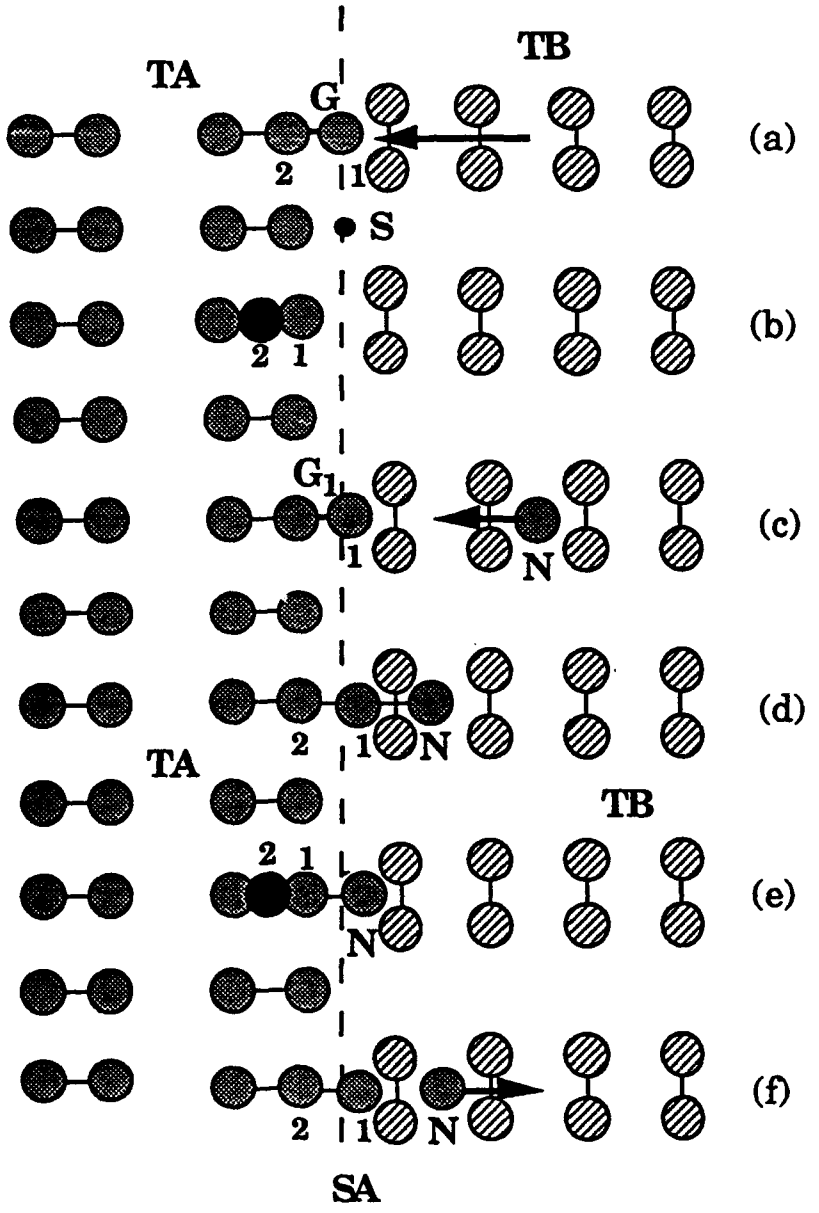

Fig. 24. The exchange mechanism by which an atom deposited on the TB terrace is transferred onto the SA terrace by climbing up the

SA step.

We can now summarize the kinetic factors that lead to the transformation of single-atom-high steps into double-atom-high ones after the deposition of half a monolayer of silicon on the surface. The first is the extreme anisotropy of adsorbate motion on the Si(100)-2X1 surface. An adatom located on top of a dimer row moves frequently along the row, and rarely in the direction perpendicular to it. This affects strongly the particle transport on terraces. An atom adsorbed on a TB terrace, on which the dimer rows are perpendicular to the step, has no trouble reaching a terrace edge. On a TA terrace the dimer rows run along the terrace and the transport of the adsorbed particles to the edge or the step is slow. This effect alone will make it difficult for the adsorbed atoms to leave the TA terraces.

The anisotropy of diffusion is only half the story. It explains the tendency of the adsorbed particles that have landed on a TA terrace to stay on the same terrace. To understand the formation of the double layer steps we must also find why and how the particles landing on the TB terraces leave them and move to the TA ones. Our calculations indicate that a particle can leave a TB terrace by climbing down (across the SB step) onto the neighboring TA terrace; the largest barrier along the way is 0.84 eV. Furthermore, the atoms adsorbed on the TB terraces can reach the SA step and engage in what we call the exchange process; as a result an adatom disappearing from the TB terrace reappears on the TA one. The barrier for the exchange process is 1.07 eV if unassisted by a second atom, and 0.54 eV if a second atom is nearby.

7. KINK-KINK INTERACTIONS IN STEP ROUGHENING

It has been observed experimentally that the single-atom-high B steps (SB) on a Si(100)-2X1 surface has kinks, while the SA steps are practically straight.[22] In Sec. 6 we have proposed that the step is rough because to a good approximation the step is formed by the independent growth of the dimer rows of the TB terrace. Here we present a thermodynamic study of roughening based on a phenomenological model for the energy of the kinks and the

interaction between them.[28] Understanding and controlling the shape of the steps is especially important because it may affect the quality of the tilted superlattices which are grown on stepped surfaces.

The work that is most significant to this section is that of Swartzentruber *et al.*,[22] who studied the statistical properties of the rough SB steps in the STM measurements. They noted that these can be reproduced rather well by a model that assumes that the energy to form a step is of the form a + b n, where n is the number of atoms in a kink (we give below a more precise definition) and a is a corner formation energy. Here we propose a slight extension of this work: we show that an energy expression that includes a kink-kink interaction term gives a slightly better fit of the data. Unfortunately there is insufficient data to decide between these two models. Future measurements of the statistical properties of the kinks as a function of temperature will be very helpful in determining the magnitude of the kink-kink interactions.

The properties of the kinks are characterized by two distribution functions: the probability N(n) of finding a kink of height n, and the probability P(s) that the distance between two neighboring kinks is s. The variables s and n are defined in the insert of Fig. 25(a). Swartzentruber *et al.*[22] have determined these two functions from the STM pictures of the B and A steps on a Si(100)-(2X1) surface. They interpreted the results by using an independent kink (IK) model which gives

$$N(n) \sim \exp[-E(n)/kT], \tag{7.1}$$

$$P(s) = p\,(1-p)^{s/2-1}. \tag{7.2}$$

Here T is the absolute temperature, $p \approx 0.44$ is the probability that a kink exists at a site along the step, and $E(n) = \varepsilon n + C$, where C is the energy of the two corners in a kink. Fitting the data for a SB step gives $\varepsilon = 0.028 \pm 0.002$ eV and $C = 0.08 \pm 0.02$ eV.

The IK model fits the data fairly well. There are however small discrepancies: (a) at low values of s the measured P(s) deviates considerably from Eq. (2); (b) for large n (≥ 16) the measured values of N(n) are higher than the values given by the IK model; (c) in the

strictly independent kink model if one walks along the step one would have equal probability to wonder upwards or downwards, while experimentally the directions of the roughening at two neighboring sites are correlated; (d) the amplitude of the roughening in a step generated by using the IK model with the parameters given above, is smaller than that of the experimental pattern.

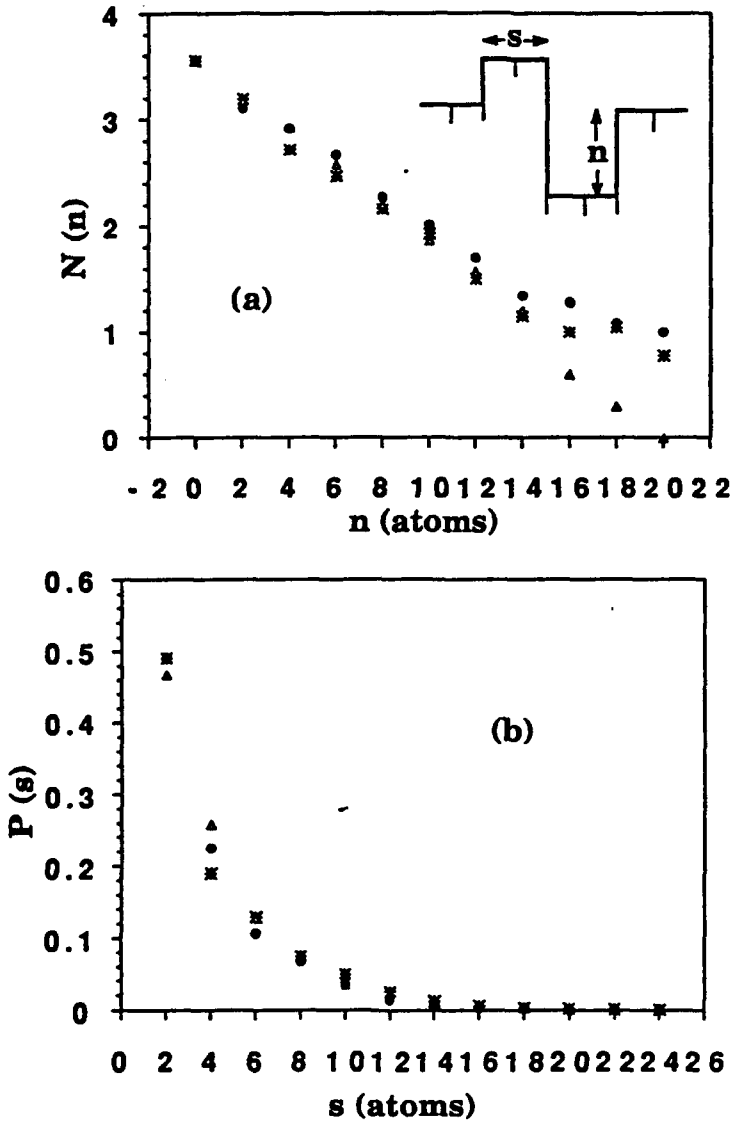

Fig. 25. (a) The kink height distribution. (b) The kink-kink distance distribution. The data from Ref. 22 is represented by stars, the soliddots and the triangles give the distributions calculated with and without kink-kink interactions, respectively.

Several recent articles have used phenomenological Hamiltonians to study the equilibrium structures of Si(100) stepped surfaces.[21,62-70] In most of these studies the interaction between steps has been taken into account, while the effects of the kink-kink interaction along a step have not been treated explicitly. Since the kink-kink distance can be much shorter along the same step than step-step separation, the interaction between the kinks may have stronger effects.

In what follows we use the Hamiltonian

$$H = \sum_{n_i} \sum_{n_j} [(|n_i| \varepsilon + C) \delta_{ij} - D (1 - \delta_{ij}) n_i n_j / s_{ij}^3], \qquad (7.3)$$

which adds to the IK expression a kink-kink interaction. The kink height n_i and the kink-kink distance s_{ij} are defined in Fig. 25(a). The kink-kink coupling strength D is positive. The sign of the product $n_i n_j$ is given by the following rule: walk along the step starting from one end and mark with arrows the direction in which you walk along the kink; each kink is thus assigned an arrow and if the arrows for the kinks i and j are antiparallel (see Fig. 26(a)) $n_i n_j < 0$; if they are parallel (see Fig. 26(b)) $n_i n_j > 0$. The kink-kink interaction gives preference to configurations in which the arrows of the neighboring kinks are parallel; thus it favors deeper kinks and smaller kink-kink separations.

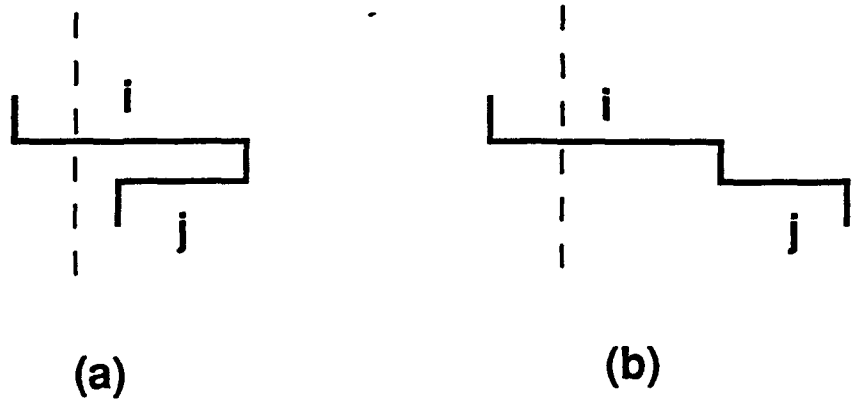

Fig. 26.

We use the $(s_{ij})^{-3}$ dependence because it is the one that gives the best agreement with the experimental data. We have also tried the forms $M\sum_{i,j} n_i n_j s_{ij}^{-2}$ and $N\sum_{i,j} s_{ij}^{-3}$ and found them less successful. There are some arguments in the literature[71] that favor a $(s_{ij})^{-3}$ dependence, but we do not find them compelling and prefer to regard our Hamiltonian as empirical. A convincing derivation of the effective Hamiltonian would obviously be valuable.

For $n_i n_j > 0$ the Hamiltonian Eq. (7.3) favors kinks with infinite height. In reality, the maximum kink height is limited by the terrace width L, so this quantity should in principle be a parameter in the theory. While adding a term limiting the maximum kink height, such as the one expressing step-step interaction, would not greatly complicate the simulations below, we find that we can fit well the existing data with the Hamiltonian (7.3). This happens because, at the temperature and angle of cut at which the data was taken, the first term in Eq. (7.3) discriminates effectively against the creation of kinks with high values of n.

The effects of the interaction term can be examined by first generating kinks on a step by Monte Carlo (MC) simulations and then calculating the distribution functions N(n) and P(s). We start with an ideal step of length 300 X (2a) where 2a is the period of translational symmetry in the direction parallel to the step, and a is the surface lattice constant on the Si(100) surface before reconstruction. Periodic boundary conditions in the direction parallel to the step are used with the period 600 a. The MC program chooses randomly a site along the step and attempts to remove two adjacent dimers from the step and place them at another randomly chosen site along the step. The Hamiltonian Eq. (7.3) is used to determine whether such a change is accepted. It takes about 200,000 moves to reach the equilibrium kink configuration. To test whether a high n cut off is necessary, to prevent the formation of kinks whose height exceeds the width of the terrace, we have rejected in our simulations attempts to create kinks with n>25 X (2a). The number of attempts rejected by this restriction is negligible, which indicates that the tendency of the kink-kink interaction to favor high n values is

statistically insignificant.

We move two dimers each time as the removal of two dimers is energetically favored: it allows the dimerization of the atoms left behind.[34]

In our simulations we have systematically examined the effects of the interaction term by varying the magnitude of D. Here we only compare the best fits of the distributions N(n) and P(s) given by the present model and the IK model, at T=600 °C. These are shown in Fig. 25. The best fitting parameters are ε = 0.029 eV, C = 0.050 eV, and D=0.0052 eV, for the present model, and ε = 0.028 eV, C = 0.063 eV, and D=0.0, for the IK model. The corner energy C = 0.063 eV obtained by us is slightly lower than the value recommended by Swartzentruber *et al.*[22] The present model agrees better with the measurements, especially for large values of n and small values of s. We have also calculated these distributions for T=500 °C, by assuming that the constants in the Hamiltonian are temperature independent, and found that they do not change significantly.

The kink-kink interaction has a greater influence on the kink-kink distance distribution P(s) for smaller s (Fig. 25(b)). The parameter set {ε, C, D} that improves the fitting of N(n) also gives a better fitting of P(s). In particular, the inclusion of the interaction term increases P(2) as compared to the value given by the IK model and diminishes the magnitude of P(s) for $s \geq 4$. These changes improve the agreement with the experiment.

In Fig. 27, we also compare the step patterns obtained for different values of D, for a terrace width L=34 X (2a), corresponding to an angle of cut of 0.3° towards [100]. As expected, the inclusion of the interaction increases thermal roughening, and also influences the global pattern of the step to favor $n_i n_j > 0$. The SB step structure shown in Fig. 27(a) (for D = 0.0052 eV) resembles more closely Fig. 1 of Ref. 22, than the pattern for D=0 (Fig. 27(b)), especially when the magnitude of the thermal roughening is considered.

Acknowledgements: We acknowledge the contribution of our collaborator Dr. Y.-T. Lu. We are grateful to Professors M. Lagally, B. Garrison, R. Hamers, D. Vvedensky and Dr. M. Wilby for sending us preprints prior to publication and for useful discussions. At Santa

Barbara we have greatly benefited from discussions with our QUEST colleagues, P. Petroff, W. Kohn, H. Weinberg and H. Kroemer. Z.Y.Z. also wishes to express his deep gratitude towards the organizers of the workshop, all the personals in the CCAST, and especially its founding director Professor T. D. Lee, for hospitality and financial assistance. This work has been supported by the National Science Foundation through the Science and Technology Center QUEST, by the NSF 87-13619 and in part by the Office of Naval Research.

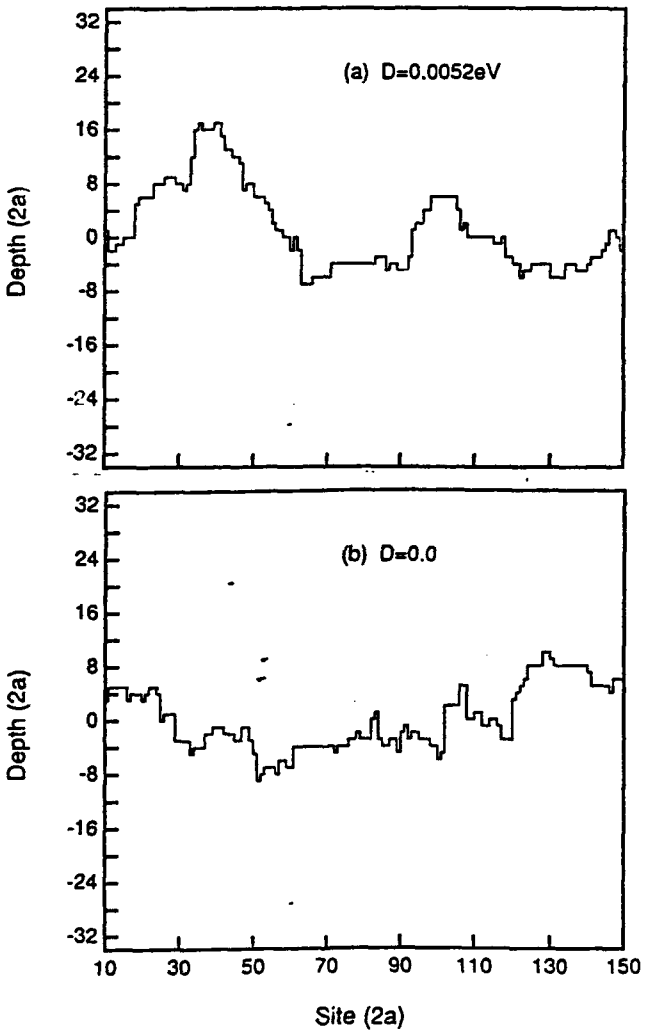

Fig. 27. The dependence of the step structure on the kink-kink interaction.

REFERENCES

1. H.-J. Gossmann and L. C. Feldman, Phys. Rev. B **32**, 6 (1985).
2. T. Sakamoto, N. J. Kawai, T. Nakagawa, K. Ohta, and T. Kojima, Appl. Phys. Lett. **47**, 617 (1985).
3. A. J. Hoeven, J. M. Lenssinck, D. Dijkkamp, E.J. van Loenen, and J. Dieleman, Phys. Rev. Lett. **63**, 1830 (1989).
4. M. G. Lagally, Y.-W. Mo, R. Kariotis, B. D. Swartzentruber, and M. B. Webb in *Kinetics of Ordering and Growth an Surfaces.* ed. M. G. Lagally (Plenum Press, New York, 1990).
5. Y.-W. Mo and M. B. Lagally, Surf. Sci. **248**, 313 (1991).
6. N. Aizaki and T. Tatsumi, Surf. Sci. **174**, 658 (1986).
7. J. Aarts, W. M. Gerits, and P. K. Larsen, Appl. Phys. Lett. **48**, 931 (1986).
8. M. Tsuchiya, P.M. Petroff, and L.A. Coldren, Appl. Phys. Lett. **54**, 1690 (1988).
9. (a) Y.-T. Lu, P. Petroff, and H. Metiu, Appl. Phys. Lett. 57, 2683 (1990); (b) Y.-T. Lu and H. Metiu, Surf. Sci. **245**, 150 (1991).
10. H.C. Kang and W.H. Weinberg, Phys. Rev. B **38**, 11543 (1988); also J. Chem. Phys. **90**, 2824 (1989).
11. M. R. Wilby, S. Clarke, T. Kawamura, and D. D. Vvedensky, Phys, Rev. B **40**, 10617 (1989); S. Clarke, M. R. Wilby, D. D. Vvedensky, and T. Kawamura, ibid. **40**, 1469 (1989); S. Clarke, M. R. Wilby, D. D. Vvedensky, T. Kawamura, K. Miki, and H. Tokymoto, ibid. **41**, 10198 (1990).
12. R. Kariotis and M. G. Lagally, Surf. Sci. **216**, 557 (1989).
13. Y. W. Mo, J. Kleiner, M. B. Webb, and M. G. Lagally, Phys. Rev. Lett. **66**, 1998 (1991).
14. T. Kawamura, T. Sakamoto, and K. Ohta, Surf. Sci. **171**, L415 (1986).
15. A detailed kinetic Monte Carlo simulation which includes the effects of dimerization and surface reconstruction is being carried out by Z. Y. Zhang and H. Metiu.
16. R. J. Hamers, U. K. Kohler, and J. E. Demuth, Ultramicroscopy **31**, 10 (1989).
17. Y. W. Mo, B. S. Swartzentruber, R. Kariotis, M. B. Webb, and M. G. Lagally, Phys. Rev. Lett. **63**, 2393 (1989).

18. P. E. Wierenga, J. A. Kubby, and J. E. Griffith, Phys. Rev. Lett. **59**, 1691 (1987).
19. F. K. Men, W. E. Packard, and M. B. Webb, Phys. Rev. Lett. **61**, 2469 (1988).
20. E. D. Williams, and N. C. Bartelt, Science **251**, 393 (1991).
21. O. L. Alerhand, *et al.*, Phys. Rev. Lett. **64**, 1691 (1990).
22. B. S. Swartzentruber, Y.-W. Mo, R. Kariotis, M. G. Lagally and M. B. Webb, Phys. Rev. Lett. **65**, 1913 (1990).
23. Z. Y. Zhang and H. Metiu, Surf. Sci. **245**, 353 (1991).
24. Z. Y. Zhang, Y.-T. Lu, and H. Metiu, Surf. Sci. **248**, L250 (1991).
25. Y.-T. Lu, Z. Y. Zhang, and H. Metiu, Surf. Sci. (1991, in press).
26. Z. Y. Zhang, Y.-T. Lu, and H. Metiu, Surf. Sci. Lett. (1991, in press).
27. Z. Y. Zhang, Y.-T. Lu, and H. Metiu, Phys. Rev. B. (1991, submitted).
28. Z. Y. Zhang, Y.-T. Lu, and H. Metiu, Surf. Sci. Lett. (1991, submitted).
29. F. H. Stillinger and T. A. Weber, Phys. Rev. B **31**, 5262 (1985).
30. T. Miyazaki, H. Hiramoto, and M. Okazaki, Jpn. J. Appl. Phys. **29**, L1165 (1990).
31. G. Brocks, P. J. Kelly and R. Car, Phys. Rev. Lett. **66**,1729 (1991).
32. D. Srivastava, and B. J. Garrison, (1990, preprint).
33. (a) J. Tersoff, Phys. Rev. B **38**, 9902 (1988). (b) J. Wang and A. Rockett, Phys. Rev. B **43**,12571 (1991).
34. D. J. Chadi, Phys. Rev. Lett. **59**, 1691 (1987).
35. F. F. Abraham and I. P. Batra, Surface Sci. **163**, L752 (1985)
36. B. W. Dodson, Phys. Rev. B**33**,7361 (1986); K. E. Khor and S. Das Sarma, Phys. Rev. B**36**,7733 (1987).
37. B. C. Bolding and H. C. Andersen, Phys. Rev. B**41**,10568 (1990).
38. K. Ragavachari, J. Chem. Phys. **83**, 3520 (1985); **84**, 5672 (1986); K. Ragavachari and V. Logovinsky, Phys. Rev. Lett. **55**, 2853 (1985); K.Ragavachari and C. M. Rohlfing, Chem. Phys. Lett. **143**, 428 (1988); J. Chem. Phys. **89**, 2219 (1988).
39. K. E. Khor and S. Das Sarma, Chem. Phys. Lett. **134**, 43 (1987).
40. E.R. Cowley, Phys. Rev. Lett. **60**, 2379 (1988).
41. J. Zi, K. M. Zhang, and X. D. Xie, Phys. Rev. B. **41**, 12915 (1990).
42. (a) P.N. Keating, Phys. Rev. **145**, 637 (1966); (b) E. Pearson, T. Takai, T. Halicioglu, and W.A. Tiller, J. Crystal Growth **70**,

(1984); (c) T. Takai, T. Halicioglu, and W.A. Tiller, Scripta Metall. **19**, 709 (1985).
43. J. Tersoff, Phys. Rev. Lett. **56**, 632 (1986).
44. R. Biswas and D.R. Hamann, Phys. Rev. Lett. 55, 2001 (1985); Phys. Rev. **B36**, 6434 (1987).
45. B.W. Dodson, Phys. Rev. **B35**, 2795 (1987).
46. D.W. Brenner and B.J. Garrison, Phys. Rev. **B34**, 1304 (1986).
47. J. Chelikowsky, J.C. Phillips, M. Kamal, and M. Strauss, Phys. Rev. Lett. **62**, 292 (1989).
48. K.E. Khor and S. Das Sarma, (a) Phys. Rev. **B36**, 7733 (1987); (b) **B38**, 3318 (1988); (c) **B39**.1188 (1989).
49. M.I. Baskes, Phys. Rev. Lett. **59**, 2666 (1987); Phys. Rev. Lett. **50**, 1285 (1983); Phys Rev. **B29**, 6443 (1984).
50. For example, E. Kaxiras and K.C. Pandey, Phys. Rev. **B38**, 12736 (1988).
51. (a) R. Car and M. Parinello, Phys. Rev. Lett. **55**, 2471 (1985); I. Stich, R. Car, and M. Parinello, Phys. Rev. Lett. **63**, 2240 (1989); (b) G. Brocks, P. J. Kelly and R. Car, Phys. Rev. Lett. **66**,1729 (1991).
52. C. Z. Wang, C. T. Chan, and K. M. Ho, Phys. Tev. Lett. **66**, 189 (1991); J. H. Wilson, J. D. Todd and A.. P. Sutton, J. Phys.: Condensed Matter, **2**, 10259 (1990).
53. W. S. Yang, F. Jona, and P. M. Marcus, Phys. Rev. B. **28**, 2049 (1983).
54. R. M. Tromp, R. J. Hamers, and J. E. Demuth, Phys. Rev. Lett. **55**, 1303 (1985); Phys. Rev.-B **24**, 5343 (1986).
55. K. Binder, ed. *Monte Carlo Methods* (Springer-Verlag, New York, 1979).
56. B. J. Garrison, M. T. Miller, and D. W. Brenner, Chem. Phys. Lett. **146**, 553 (1987).
57. D. Srivastava, B. J. Garrison, and D. W. Brenner, Phys. Rev. Lett. **63**, 302 (1989).
58. For simplicity, the three F sites found in Ref. 24 are treated here as one site. We can do so because the barriers between these sites are very small.
59. A. F. Voter and J. D. Doll, J. Chem. Phys. **82**, 80 (1985).
60. Z. Y. Zhang, K. Haug, and H. Metiu, J. Chem. Phys. **93**, 3614

(1990).
61. J. D. Weeks and G. H. Gilmer, Adv. Chem. Phys. 40, 157 (1979).
62. O. L. Alerhand, D. Vanberbilt, R. D. Meade, and J. D. Joannopoulos, Phys. Rev. Lett. **61**, 19731 (1988).
63. R. Kariotis, B. S. Swartzentruber, and M. G. Lagally, J. Appl. Phys. **67**, 2848 (1990).
64. S. Stoyanov, Europhys. Lett. **11**, 361 (1990).
65. T. W. Poon, S. Yip, P. S. Ho, and F. F. Abraham, Phys. Rev. Lett. **65**, 2161 (1990).
66. N. C. Bartelt, T. L. Einstein, and E. D. Williams, Surf. Sci. **240**, L591 (1990).
67. N. C. Bartelt, T. L. Einstein, and C. Rottman, Phys. Rev. Lett. **66**, 961 (1991); O. L. Alerhand, A. N. Berker, J. D. Joannopoulos, D. Vanberbilt, R. J. Hamers, and J. E. Demuth, Phys. Rev. Lett. **66**, 962 (1991).
68. R. Kariotis and M. G. Lagally, Surf. Sci. **248**, 295 (1991).
69. R. Kariotis, Surf. Sci. **248**, 306 (1991).
70. L. Barbier, A. Khater, B. Salanon, and J. Lapujoulade, Phys. Rev. B. **43**, 14730 (1991).
71. V. I. Marchenko and A. Ya. Parshin, Zh. Eksp. Teor. Fiz. **79**, 2576 (1980) [Sov. Phys. JETP **52**, 129 (1980)]; K. H. Lau and W. Kohn, Surf. Sci. **65**, 607 (1977).

TECHNICAL REPORT DISTRIBUTION LIST - GENERAL

Office of Naval Research (2)*
Chemistry Division, Code 1113
800 North Quincy Street
Arlington, Virginia 22217-5000

Dr. James S. Murday (1)
Chemistry Division, Code 6100
Naval Research Laboratory
Washington, D.C. 20375-5000

Dr. Robert Green, Director (1)
Chemistry Division, Code 385
Naval Air Weapons Center
Weapons Division
China Lake, CA 93555-6001

Dr. Elek Lindner (1)
Naval Command, Control and Ocean
Surveillance Center
RDT&E Division
San Diego, CA. 92152-5000

Dr. Bernard E. Douda (1)
Crane Division
Naval Surface Warfare Center
Crane, Indiana 47522-5000

Dr. Richard W. Drisko (1)
Naval Civil Engineering
Laboratory
Code L52
Port Hueneme, CA 93043

Dr. Harold H. Singerman (1)
Naval Surface Warfare Center
Carderock Division Detachment
Annapolis, MD 21402-1198

Dr. Eugene C. Fischer (1)
Code 2840
Naval Surface Warfare Center
Carderock Division Detachment
Annapolis, MD 21402-1198

Defense Technical Information
Center (2)
Building 5, Cameron Station
Alexandria, VA 22314

* Number of copies to forward